Published in final edited form as:
Prog Nucleic Acid Res Mol Biol. 2008 ; 82: 147–197. doi:10.1016/S0079-6603(08)00005-6.

Site-directed spin labeling studies on nucleic acid structure and dynamics

Glenna Z. Sowa and **Peter Z. Qin**
Department of Chemistry, University of Southern California, Los Angeles, California 90089

Abstract

Site-directed spin labeling (SDSL) uses electron paramagnetic resonance (EPR) spectroscopy to monitor the behavior of a stable nitroxide radical attached at specific locations within a macromolecule such as protein, DNA, or RNA. Parameters obtained from EPR measurements, such as internitroxide distances and descriptions of the rotational motion of a nitroxide, provide unique information on features near the labeling site. With recent advances in solid-phase synthesis of nucleic acids and developments in EPR methodologies, particularly pulsed EPR technologies, SDSL has been increasingly used to study the structure and dynamics of DNA and RNA at the level of the individual nucleotides. This chapter summarizes the current SDSL studies on nucleic acids, with discussions focusing on literature from the last decade.

I. Overview

In site-directed spin labeling (SDSL) (1), a nitroxide molecule (spin label) is covalently attached at a specific site within a macromolecule such as protein, DNA, or RNA (Fig. 1). Electron paramagnetic resonance (EPR) spectroscopy is used to characterize the behavior of a chemically inert, unpaired electron that is localized at the nitroxyl group of the nitroxide. Structural and dynamic features at the attachment site are inferred from EPR measurements (Fig. 1). In protein studies, SDSL has matured as a tool for studying the structure– function relationship, and has been used to provide information at the level of the protein backbone (2–8). SDSL is useful in studying high molecular weight systems under physiological conditions. It has been particularly successful in studying systems (e.g., membrane proteins) that are difficult to investigate using other methods, such as X-ray crystallography and NMR spectroscopy (2–8).

SDSL has been used to study nucleic acids, and data suggest that one can obtain unique structural and dynamic information about DNA and RNA at the level of individual nucleotides (9). Use of nitroxides to study nucleic acids was first reported in the 1970s (10). In the 1970s and 1980s, studies were done using DNA and RNA that were uniformly labeled with nitroxides (11), as well as using tRNAs labeled at naturally occurring modified nucleotides (12,13). In the 1980s and 1990s, with developments in solid-phase chemical synthesis, nitroxides were incorporated site-specifically into DNA strands, and EPR was used to study DNA duplexes (11,14). In the last decade, a number of methods were reported for attaching nitroxides at specific sites within RNA strands, and SDSL was used to study folded RNA molecules (9).

The majority of nucleic acid SDSL studies used one of two types of EPR measurements (Fig. 1) (9). Distance measurements between pairs of nitroxides provide direct structural constraints in nucleic acid systems. In addition, the mobility of a single-labeled nitroxide can be measured to yield structural and dynamic information at the labeling site. Because nucleic acids are different from proteins in the nature of the basic chemical constituents (4 nucleotides vs 20 amino acids) and their secondary structural units (B-form/A-form doubled-stranded helix vs α-helix/β-sheet), SDSL of nucleic acids requires unique methodologies, particularly in the

areas of nitroxide attachment and the correlation of the nitroxide behavior to that of the parent molecule.

In this chapter, we summarize the current state of the use of SDSL to study nucleic acids, with the discussions focusing primarily on literature from the last decade. The physical principles underlying EPR measurements are first described, followed by an overview of available methods for site-specific attachment of nitroxides to nucleic acids. Then we discuss the use of distance measurements and nitroxide spectral lineshape analysis to study nucleic acids. We conclude with a brief overview of possible future directions in nucleic acid SDSL.

II. Basic Physics Underlying SDSL

A spin label is a molecule that has at least one unpaired electron. Nitroxides, such as those containing a moiety of either *R* = 1-oxyl-2,2,5,5-tetramethyl-3-pyrroline (with a five-membered unsaturated ring) or *R′* = 1-oxyl-2,2,6,6-tetramethylpiperidine (with a six-membered saturated ring) (Fig. 1), are commonly used as spin labels in studies of proteins and nucleic acids. These probes are stable radicals and contain one unpaired electron that localizes primarily within the nitroxyl group (15). This unpaired electron has a spin quantum number $S = 1/2$. The physics describing the behavior of this unpaired electron in the presence of a magnetic field is analogous to that of proton NMR describing the behavior of a proton (nuclear spin $I = 1/2$) in the presence of a magnetic field. In this section, we outline the basic physics necessary to understand SDSL. The readers are referred to several excellent books and review articles for more detailed descriptions of the physics relevant to SDSL (4,8,16–18).

A. The Zeeman and Hyperfine Interaction

The Zeeman interaction is the interaction between an external magnetic field and the magnetic moment of an electron. The magnetic dipole moment of an electron (μ_e) is related to its spin (S)

$$\mu_e = g\beta_e S \tag{1}$$

where β_e is the Bohr magneton (the intrinsic unit of an electron magnetic moment, $\beta_e = 9.274 \times 10^{-24}$ J T^{-1}), and g is the electron spin g-factor. The g-factor of a nitroxide is very close to that of a free electron ($g_e \sim 2.0023$).

In the presence of a static magnetic field B_0, an electron occupies one of two states, which can be thought of as the electron aligning with or against the magnetic field. These two states are described by the quantum number S_z which is the projection of the electron spin angular momentum (S) on an arbitrary axis, z (usually chosen as the direction of the external magnetic field B_0). The nitroxide has $S_z = +1/2$ or $S_z = -1/2$, and the energy of each state can be written as

$$E = \mu B_0 = g\beta_e S_z B_0 \tag{2}$$

The energy difference, ΔE between these two states depends on the strength of the magnetic field, and can be expressed as

$$\Delta E = g\beta_e B_0 \tag{3}$$

At resonance, the electron absorbs energy from the external electromagnetic radiation. The resonance condition is defined by

$$\Delta E = g\beta_e B_0 = h\upsilon \tag{4}$$

where h is the Planck constant ($h = 6.626 \times 10^{-34}$ J s)and ν is the frequency of the electromagnetic radiation. Notice that the electron magnetic moment ($\mu_e = 9.285 \times 10^{-24}$ J T^{-1}) is 658 times larger than the proton magnetic moment ($\mu_p = 1.411 \times 10^{-26}$ J T^{-1}). This gives rise to a high sensitivity in EPR detection compared to NMR.

When the resonance condition is met, electrons can be promoted from a low energy state ($S_z = -1/2$) to a higher energy state ($S_z = +1/2$), and absorption of the microwave radiation occurs (Fig. 2). This is the basis of the continuous-wave (cw) EPR measurement. Conventionally, the cw-EPR spectrum is measured by sweeping the external magnetic field (B_0) at a fixed microwave frequency. Most studies are done in the X-band, with the microwave frequency at ~9.5 GHz and resonance occurring at B_0 ~ 3400 Gauss (0.34 T). Spectrum is generally obtained using source modulation and the lock-in amplification technique, which increases the signal-to-noise ratio (4,16). The resulting spectrum is the first derivative of the absorption spectrum (Fig. 2B).

In addition to the Zeeman effect, the unpaired electron also experiences a small local magnetic field produced by nearby nuclei. This is known as the hyperfine interaction, and may counter or enhance the externally applied field. In a nitroxide, the dominant hyperfine interaction is between the unpaired electron and the ^{14}N nucleus of the nitroxyl group. The $I = 1$ ^{14}N nucleus splits the nitroxide EPR signal into $2I + 1 = 3$ lines, each corresponding to a ^{14}N nuclear spin state ($m_I = -1, 0, +1$) (Fig. 2A). The resonance condition is modified to include the hyperfine interaction, A

$$h\upsilon = g\beta_e B_0 + m_I A \tag{5}$$

The hyperfine interaction is due to the dipolar interaction between the electron spin and the nuclear spin, and includes both isotropic and anisotropic components. The isotropic component is proportional to the electron spin density at the nitrogen and the oxygen nucleus of the nitroxyl group. The anisotropic components arise from the orientation dependence of the electron–nuclei interactions due to the asymmetric orbital of an unpaired electron. For example, the dipolar interaction is stronger when the orbital z-axis is aligned with the external field, and weaker when the alignment is perpendicular. In fact, the Zeeman interaction is also anisotropic, as the asymmetric orbital results in orientation dependence in the g-factor.

Rotational motions of the nitroxide (dynamics) lead to averaging between the elements of the g tensor and the A tensor, and give rise to variations in the observed cw-EPR spectrum. When the nitroxide dynamics are coupled to the macromolecule, the cw-EPR spectrum can be used to infer information about the local environment around the labeling site (see Section V).

B. The Dipolar Interaction Between a Pair of Electron Spins

When the dipolar interaction between electron spins A and B is considered, an E_{dip} term is added to each electron energy level (32,80):

$$E_{\mathrm{dip}}=D_{\mathrm{dip}}\cdot S_{z}^{A}\cdot S_{z}^{B}\cdot\frac{(1-3\cos^{2}\theta)}{r_{\mathrm{AB}}^{3}} \tag{6}$$

and

$$D_{\mathrm{dip}}=\frac{\mu_{0}g_{\mathrm{A}}g_{\mathrm{B}}\beta_{\mathrm{e}}^{2}}{4\pi}=h\nu_{\mathrm{dip}} \tag{6a}$$

where μ_0 is the vacuum permeability, r_{AB} is the distance between spin A and spin B, and θ is the angle between the distance vector $\mathbf{r}_{AB}$ and the external magnetic field $\mathbf{B}_0$ (Fig. 3A). D_{dip} represents the dipolar splitting of an EPR transition. When $g_A = g_B = 2$, the dipolar frequency ν_{dip} = 51921 (MHz)·(Å^3) (32,80).

Eq. 6 indicates that the dipolar interaction depends on θ. When $\mathbf{r}_{AB}$ adopts a static and isotropic distribution with respect to $\mathbf{B}_0$, all θ values are equally populated. This yields a Pake Pattern (Fig. 3B) (19). On the other hand, if the frequency of the spin pair rotation is rapid relative to ν_{dip}, no net dipolar interaction can be observed.

III. Site-Specific Attachment of Nitroxides to Nucleic Acids

The first step in SDSL is to attach a nitroxide at a specific site within the macromolecule (Fig. 1). In protein studies, the residue at the intended labeling site is generally mutated to a cystein, and a thiol-reactive nitroxide derivative is then reacted with the cystein −SH group (1,2,8). This strategy cannot be applied directly to nucleic acids. There are 4 common nucleotides compared to 20 amino acids, and these nucleotides do not contain functional groups that are reactive under conditions compatible with nucleic acid stability (i.e., aqueous solution and physiological pH).

Currently, the most efficient spin labeling strategies rely on solid-phase chemical synthesis to achieve site-specific attachment of the nitroxide (Table I). Solid-phase chemical synthesis of nucleic acids, primarily based on phosphoroamidite chemistry (20,21), assembles either DNA or RNA strands from the 3′ to the 5′ direction one nucleotide at a time. It is possible to modify the synthesis cycle to introduce a modification at a specific nucleotide. The modified nucleotide may contain a reactive functional group (such as −SH or $-NH_2$), which can be further derivatized with nitroxide. Alternatively, the modified nucleotide may include a nitroxide moiety. Current state of the art solid-phase synthesis is capable of routinely synthesizing DNA oligonucleotides that are approximately 100-nucleotide (nt) long and RNAs that are approximately 50-nt long. Methods have been reported to attached nitroxides to specific phosphate (22), sugar (23,24), and base positions (25-34) within a chemically synthesized DNA or RNA oligonucleotide (Table I). These methods will be discussed in Section III.A.

Currently, there is no general enzymatic approach to substitute one nitroxide-modified nucleotide at a given site within a DNA or RNA. Enzymatic incorporations of nitroxides at the terminus of nucleic acids as well as at a limited number of internal positions of particular systems have been reported. These methods will be discussed in Section III.B.

A. Nitroxide Labeling Methods Relying on Solid-Phase Chemical Synthesis

1. Nitroxide Labeling at a Specific Internal Phosphate Site—A phosphate group is present in every nucleotide, and is an ideal site for the attachment of a nitroxide at any desired

nucleotide within a nucleic acid sequence. Qin *et al*. have reported a phosphorothioate scheme for attaching a nitroxide to a specific modified phosphate position in DNA or RNA (Table I, entry 1) (22,35–37). There is also a report where an H-phosphonate modification was used to attach a nitroxide to a nucleotide near the 5′ terminus of DNA (38).

In the phosphorothioate scheme, the phosphate group at the desired labeling site is modified to a phosphorothioate (substituting a sulfur for one of the nonbridging oxygens) during solid-phase chemical synthesis (22). The phosphorothioate containing oligonucleotide is reacted with an iodomethyl derivative of a nitroxide. The product is a nitroxide linked to the phosphorous of the oligonucleotide by a thioether bond. This nitroxide is designated as R5, and a detailed labeling protocol has been recently published (37).

The phosphorothioate labeling scheme targets a functional group that is present in all nucleotides. Therefore, the same chemistry can be used to attach a nitroxide to any nucleotide position within an arbitrary DNA or RNA sequence. This enables one to efficiently conduct nitroxide scanning, where the probe is systematically attached to different positions in a given DNA or RNA sequence. Studies have demonstrated that R5 labeling is 90–100% efficient (22,35,36), and that the presence of R5 does not severely perturb the conformation of DNA and RNA duplexes (35,36). The cost of introducing a phosphorothioate is less than 1/20 of the cost of adding a modified nucleotide, and R5 labeling is a one-step reaction in the aqueous solution. These features facilitate spin labeling of large molecules. The phosphorothioate scheme has been demonstrated on a 68-nt-long DNA (MW ~ 21 kDa) (35).

There are several additional features of R5 that should be taken into account when designing an experiment (37). First, the pyrroline ring is linked to the nucleic acid (represented by the phosphorous atom at the labeling site) through three rotatable single bonds (Table I, entry 1). While such flexibilibty may minimize the effect of the nitroxide on the local structure of the parent molecule, there is not a uniform, direct correlation between the the location of the nitroxide and the attachment point at the parent molecule. Second, solid-phase synthesis introduces two phosphorothioate diastereomers (R_p and S_p) in an approximately 50/50 ratio, and nitroxides attached to different disastereomeric centers at the same nucleotide may experience different local environments. In short oligonucleotides (up to ~15 nt), the diastereomers can be separated using HPLC (37,82), and one can carry out SDSL studies on either mixed diastereomers or on pure diastereomers (82, Popova and Qin, manuscript in preparation). Third, at the R5-labeled nucleotide, one negative charge at the phosphate group is lost, which may pose problems at certain labeling sites or in some studies (e.g., electrostatic measurements). Finally, when using the phosphorothioate scheme to label RNA, one has to remove the 2′-hydroxyl group adjacent to the phosphorothioate to prevent strand scission upon labeling (37). This may lead to additional perturbation to the structure, dynamics, and function of the parent molecule.

The R5 nitroxide has been used to measure distances in both DNA and RNA (35,36) (Section IV.B), and an efficient computation program has been established to interpret the measured distances based on the structure of the parent molecule (37,39) (Section IV.C.1). Together these provide the necessary elements for using R5 to map the global structure (as defined by the relative positioning of helical axes) of nucleic acids. In addition, studies have shown that cw-EPR spectra of nitroxides labeled using the phosphorothioate scheme can provide information on the local environment in DNA and RNA (Popova and Qin, manuscripts in preparation).

2. Attaching Nitroxide at the 2′ Position of the Sugar—Schemes for attaching a nitroxide to the 2′ position of the sugar of RNA have been reported by the Sigurddsson (23) (Table I, entry 2a) and DeRose groups (24) (Table I, entry 2b). In these schemes, a modified phosphoroamidite containing a 2′-NH_2 group is substituted at the desired labeling site. The 2′-

NH_2 group is then reacted with an amine-reactive nitroxide derivative. This connects the nitroxide to the sugar of the nucleotide by a semirigid linker (Table I, entry 2).

Attachment of a nitroxide at the 2′-sugar position does not significantly alter the structure and function of the RNA (23,24). Distance measurements (24,40) (Section IV.A) and EPR lineshape analysis (Sections V.D.4 and V.D.5) have been used to study RNA in this fashion (23,41–45). In principle, this labeling scheme can be applied regardless of the base identity. However, incorporating 2′-NH_2-modified purines (A and G) is difficult, and currently this labeling scheme has only been used to attach nitroxides to specific uridine (23,24) and cytosine nucleotides (44) within RNAs.

3. Nitroxide Labeling at base Positions—The reported methods for attaching nitroxides to nucleic acid bases can be grouped into three classes. One set of methods attaches nitroxides postsynthetically to an oligonucleotide containing a modification at one specific base. The second group of methods involves on-column nitroxide derivatization during chemical synthesis. The third group of methods directly incorporates nitroxide-containing phosphoramidites into nucleic acid strands.

The postsynthetic derivatization approach uses a similar strategy to that used in backbone (Section III.A.1) and sugar labeling (Section III.A.2). Two groups have reported introducing a 4-thio uridine (4-thioU) at specific sites within RNA oligonucleotides, and then labeling the RNA with various thio-reactive nitroxides (Table I, entry 3) (31, 46). The 4-thioU method has been used to probe structural and dynamic features of folded RNA (31) (Section V.D.3) and to obtain long-range distance constraints in protein/RNA complexes by measuring the paramagnetic relaxation enhancement (PRE) effects (46–49) (Section VI.C). The 4-thioU scheme has the advantage that the coupling between the nitroxide and the oligonucleotide can be carried out at near physiological pH in aqueous solution. However, upon nitroxide labeling at the 4-position of the uridine base, the N3 proton is lost (Table I, entry 3), which affects the Watson-Crick base-pairing between A and U (31).

Another class of base labeling methods uses an on-column derivatization strategy. The nitroxide is reacted with the modified base during the solid-phase chemical synthesis, and the labeled oligonucleotide is separated from the reagents and by-products in the wash step during chemical synthesis. Schiemann *et al.* have used this approach to attach nitroxides to 5-iodouridine, 5-iodocytidine, and 2-iodoadenine (Table I, entry 4) (32, 34, 50, 51). The resulting nitroxide moiety does not interfere with Watson-Crick base pairing, and is rigidly attached to the base with an acetylene bond. Long-range distance measurements using this class of nitroxides have been demonstrated in both DNA (32) and RNA (34, 50) (Section IV.B). However, during chemical synthesis, the nitroxide is exposed to various chemicals as it goes through multiple synthesis cycles and deprotection steps. This may lead to undesired products such as reduced nitroxides that have no EPR signal (32, 34, 50).

The third class of methods directly inserts a nitroxide-containing phosphoroamidite into the oligonucleotide during chemical synthesis. In the 1980s and 1990s, Bobst *et al.* synthesized a series of nitroxide-modified 2′-deoxy pyrimidine nucleosides, where the nitroxide moiety was tethered to the C-5 positions by linkers of various lengths and flexibilities (see two examples in Table I, entry 5) (11). These modified nucleosides are subsequently converted to building blocks used in solid-phase chemical synthesis, and are incorporated into DNA strands (Section V.D.2) (11). Hopkins *et al.* synthesized oligonucleotides using a phosphoroamidite called T^*, in which the nitroxide is linked to the base by an acetylene bond (Table I, entry 4a) (27). Recently, Gannett *et al.* reported a simplified scheme for the synthesis of a T^* variant that contains a six-membered ring nitroxide (30).

Hopkins *et al.* developed a heavily modified nucleoside called dQ (Table I, entry 6a) after their work on T^* (28). dQ has a nitroxide fused to an oxoquinoline and can base pair with 2-aminopurine. It has been used extensively in studying DNA duplexes (Section V.D.2). Very recently, Sigurdsson *et al*. reported a new probe, **Ç** (C-spin), in which the nitroxide is fused to a phenoxazine derivative (Table I, entry 6b) (33). This modified nucleoside can form hydrogen bond with a guanine in the same fashion as that of a Watson-Crick G/C pair. Upon reduction of the nitroxide, **Ç** is found to be highly fluorescent (33), allowing multiple studies to be done on the same sample. However, synthesis of both dQ and **Ç** is very challenging, and currently has only been reported for DNA.

B. Nitroxide Labeling Using Enzymatic Methods

1. Nitroxide Labeling at the Nucleic Acid Terminus—Grant and Qin recently reported a 5ps labeling scheme for nitroxide labeling at the 5′ terminus of arbitrary sized nucleic acids (52). In this method, T4-polynucleotide kinase was used to enzymatically substitute a phosphorothioate group at the 5′ terminus of either DNA or RNA. The resulting phosphorothioate was reacted with an iodomethyl derivative of a nitroxide. The method was successfully demonstrated on both chemically synthesized and naturally occurring nucleic acids. Duplex formation and tertiary folding of nucleic acids were observed using these nitroxide labels.

Shin *et al.* reported a method for attaching nitroxides to the 5′ terminus of RNAs synthesized by the T7 RNA polymerase (53). In this method, a modified nucleotide, guanosine 5′-*O*-(3-thiomonophosphate) (GMPS), is added to a mixture of unmodified nucleoside triphosphates. T7 RNA polymerase places GTP or GMPS at the 5′ terminus of the RNA transcript, but incorporates only GTP at the subsequent internal positions. With a large excess of GMPS to GTP (3:1), a majority of the RNA transcripts possesses a 5′ phosphorothioate instead of a 5′ triphosphate, and the phosphorothioate group is subsequently reacted with a thiol-reactive nitroxide derivative.

Labeling at the 3′ terminus was reported on tRNA (54). In this method, the ribose at the 3′ terminus was oxidized with periodate, and then reacted with a hydrazine derivative of nitroxide. However, this method cannot be applied directly to DNA.

2. Enzymatic Incorporation of Nitroxide-Modified Nucleotides—A number of nitroxide-labeled nucleotide triphosphates (NTPs) have been reported to serve as acceptable substrates for nucleic acid-synthesizing enzymes. For example, Bobst and co-workers synthesized a variety of triphosphate derivatives of modified uridine, deoxyuridine, and deoxycytidine, in which the nitroxide is attached to the 5 or 4 position of the base by flexible tethers (e.g., Table I, entry 5) (11). Most of these nitroxide-modified NTPs were successfully incorporated into nucleic acid strands by enzymes, including template-independent enzymes, such as terminal deoxynucleotide transferase (55), or template-dependent enzymes, such as DNA polymerase I from *Escherichia coli*. (56) and Taq polymerase (57). Studies found that nitroxide-modified NTPs with 1–2 atom tethers do not incorporate well, indicating that some flexibility in the tether is required (11).

Perhaps the biggest challenge in enzymatic incorporation of nitroxides is to achieve site-specificity. For example, one can attach nitroxides to all Ts within a given DNA sequence by replacing dTTP with a nitroxide-labeled deoxyuridine triphosphate, or one can randomly replace a certain percentage of Ts by mixing dTTP and the nitroxide-labeled variant. However, to replace only one specific T, one generally has to pick a sequence that has only one T present (58). This limits experimental design.

C. Future Developments

In general, the chemical synthesis approach allows one to direct the nitroxide to a specific location, but is limited by the size of the DNA and RNA that can be synthesized. The enzymatic method is more suitable for large DNA and RNA molecules, but it is difficult to place the nitroxide at one specific internal site. Combining the two approaches may allow site-specific nitroxide labeling of large DNA and RNA molecules, and should be explored in the future.

IV. Distance Measurements Using SDSL

In SDSL, internitroxide distance measurements provide structural constraints, which can be used to determine the global structure of a macromolecule and to monitor conformational changes. SDSL distance measurements do not require crystalline samples and are not limited by the molecular weight of the system. This makes SDSL useful for systems that are difficult to study using X-ray crystallography or NMR spectroscopy.

While both SDSL and flouroscence resonance energy transfer (FRET) use a pair of molecular probes to measure distances in macromolecules, there are a number of features that distinguish SDSL from FRET. In SDSL, distances are measured using a pair of chemicially identical nitroxide probes, which simplifies the labeling procedure as compared to attaching two chemically distinct fluorophores. Nitroxides are smaller than most fluorophores, causing less structural perturbation as compared with larger probes. As shown in Eq. (6), EPR measurements explicitly account for the angle (θ) between the internitroxide distance vector and the external magnetic field, whereas in FRET, a complete average of the angular dependence is generally assumed. Interpretation of distances measured using SDSL is also facilitated by the fact that the unpaired electron is localized to the nitroxyl group in a nitroxide (15), whereas relationships between the dipole moment and the chemical structure of the label vary with the choice of fluorophophore. On the other hand, single-molecule FRET measurements in biological systems are now routine, while single-molecule detection of electron spins is still being developed (59).

The fact that a nitroxide is an extrinsic molecular probe has important implications in distance measurement and data analysis and interpretation. Hustrdt and Beth have categorized the majority of SDSL distance measurements into three cases (60,61). In the first case, called statically arranged spins, each nitroxide adopts a unique conformation with respect to the parent macromolecule, while rotational reorientation of the macromolecule can be treated as static on the EPR timescale (rotational correlation time is 1 μs or longer for X-band EPR). This means that there is a unique internitroxide distance vector with respect to the macromolecule. The magnitude and orientation of this vector can be determined analytically (62). However, most studies of proteins and nucleic acids do not fall into this category due to nitroxide motions.

In the second case, the macromolecule can be treated as static on the EPR timescale, and a distribution is observed in both the magnitude and the orientation of the internitroxide distance vector. This case, called statically disordered spins, describes the majority of SDSL distance measurements in proteins and all reported studies in nucleic acids. The goal is then to describe a distance and orientation distribution $P(r, \theta)$ that best models the true distribution and provides the best fit to experimental data. The determination of $P(r, \theta)$ may be limited by both theoretical and experimental factors such as available information on nitroxide conformer distributions, noise in the experimental data, and the number of parameters that can be uniquely determined.

The third case is when the nitroxides or macromolecules or both are undergoing significant rotational reorientation on the EPR timescale. These motions partially or completely average the dipolar interaction, resulting in a reduction or elimination of observable dipolar interaction effects. An example in this case has been reported in SDSL distance measurements in the

protein T4 lysozyme (63), where global tumbling of the small protein leads to complete averaging of the dipolar interaction. In this study, it was shown that perturbations due to dipolar interactions give rise to line broadening in the cw-EPR spectrum. The amount of broadening has a $1/r^6$ dependence on the internitroxide distance (63).

In the following sections, we will describe distance measurements in nucleic acids using cw-EPR (Section IV.A) and pulsed EPR (Section IV.B). Pulsed EPR techniques are used to measure distances between approximately 20 and 80 Å, whereas cw-EPR is used to measure distances below 25 Å. Reported methods for correlating measured internitroxide distances to the stucture of the parent molecule will be discussed in Section IV.C.

A. Short-Range Distances Measured Using cw-EPR

Continuous wave EPR (cw-EPR) measures the absorption of external radiation by an unpaired electron, which is determined by the electron's spin energy levels (section II.A). The electron-electron dipolar interaction can be thought of as a perturbation to the energy levels of the non-interacting spin, and therefore, this interaction affects the cw-EPR spectrum. At a distance of 25 Å, dipolar interaction splits EPR absorption lines by ~ 2 Guass (64,65). This is small compared to the cw-EPR spectrum linewidth of a frozen ^{14}N nitroxide, and is difficult to measure. Therefore, cw-EPR measures distances < 25 Å.

All reported cw-EPR distance measurements in nucleic acids are examples of statically disordered spins, with the dipolar interaction manifesting itself as an overall spectral broadening (24,53). To use cw-EPR to measure the dipolar interaction between sites A and B of a macromolecule, three spectra should ideally be measured. These three spectra are of nitroxides attached to site A only, to site B only, and simultaneously to A and B. By comparing the lineshape of the double-labeled spectrum (labels at both A and B) to the sum of the two single-labeled spectra (A only + B only), the broadening function can be determined. Distances can be determined from these measurements using deconvolution (64–66) or convolution (67) methods.

There are two reports in the nucleic acid literature on cw-EPR distance measurements. Shin *et al.* measured distances between the HIV Rev peptide and the Rev response element (RRE) RNA (53). One nitroxide was attached to a fixed residue within the Rev peptide, and the other nitroxide was attached to 5′ terminus of the RNA using the GMPS scheme (Section III.B.1). A combination of circular permutation and mutation was used to move the 5′ terminus of the RNA to three different locations within the tertiary structure. The three measured distances are in agreement with the available structures of the RRE/Rev complex (53). DeRose *et al.* used nitroxides attached to 2′-sugar positions of specific uridines (Table I, entry 2b) to measure distances in RNA (24). Measurements in a 10-mer of RNA were found to be in qualitative agreement with values expected based on an idealized A-form duplex. Furthermore, cw-EPR distance measurements were used to study ion-dependent conformational changes in the TAR RNA (24).

Distances measured using cw-EPR are technologically simple, but are limited to distances <25 Å. cw-EPR may be most suitable for structural probing in a local region, as well as for monitoring conformational changes in which some or all distances involved are less than 25 Å. To ensure that the condition of statically disordered spins was met, the reported nucleic acid studies measured samples in a frozen glassy state (24,53). However, it is also possible to measure distances in samples at room temperature (66).

B. Nanometer Distances Measured Using Pulsed EPR

Pulsed EPR uses short (ns) but intense (kW) pulses of microwave radiation to probe the behavior of the unpaired electron(s), providing much better spectral and time resolution than cw-EPR (68). While the theory and technology of pulsed EPR is closely related to that of modern (pulsed) NMR spectroscopy, EPR specific modifications are required due to unique features of electron spins, such as their large magnetic moment and short relaxation time (approximately three orders of magnitude shorter in EPR than in NMR) (68). Currently, a commercially available pulsed EPR spectrometer (e.g., ELEXSYS E580 from Bruker Biospin, Inc.) is capable of repeated detection (every 1 s) of tiny signals (<1 nW) that occur tens of nanoseconds, after a powerful (>1 kW) applied microwave pulse. More powerful instrumentation is also being developed (69). This will provide many opportunities to use pulsed EPR in studying biological systems (68).

A number of EPR pulse schemes have been developed for measuring distances between two paramagnetic centers (70–79) [see also a recent review by Schiemann and Prisner (80)]. These schemes aim to achieve precise distance measurements by completely separating the electron dipolar interaction from all other interactions. Two general classes of pulse schemes have been used to measure distances in nucleic acids. One class of methods, developed by the Freed group, measures dipolar interactions by monitoring the time-dependence in the generation of double-quantum coherence (DQC) involving both spins (5,69,75,76,78,81). The measurements use strong, nonselective pulses to excite all radical populations in the system. The DQC signal shows an oscillating pattern with the oscillation frequency giving a direct measurement of the dipolar interaction. DQC schemes with 4, 5, and 6 pulses have been developed (69). A variant of the six-pulse scheme, called double-quantum filtered refocused electron spin echo, has been used to measure a distance in a 26-base-pair RNA duplex (81). In this study, the nitroxides were attached to two 4-thioU bases located at the termini of the duplex, and a distance of 72 Å was measured. This represents the longest measured distance reported in nucleic acids to date.

Another pulsed EPR method, based on electron–electron double resonance (ELDOR) techniques, has been applied to measure distance in a number of DNA and RNA systems (32,34–36,40,83). In ELDOR measurements, the sample is irradiated with microwave pulses at two frequencies, called the observer and pump frequencies, corresponding to two different regions of the EPR spectrum (see Fig. 4 for an example). The spectral region corresponding to the observer frequency is monitored, and any pump pulse-dependent change is called an ELDOR response.

The dipolar interaction between electron spins is one of the mechanisms that give rise to an ELDOR signal. One ELDOR scheme that allows selective measurement of the dipolar interaction is pulsed double electron–electron resonance (DEER, also referred to as pulsed ELDOR). The first published DEER scheme used a three-pulse sequence that was based on a method for detecting nuclear spin coupling (the Hahn sequence) (70,72). An extended four-pulse DEER scheme was subsequently developed and has the advantage of being able to provide dead-time free time domain data (79,84). The pulse scheme for the four-pulse DEER is shown in Fig. 4. At the observer frequency (v_1), a refocused echo with a fixed position in time is detected for spins in resonance (defined as spin A). Between the second and third v_1 pulses, an inversion pulse is applied at the pump frequency (v_2), which flips spins that are in resonance with v_2 (defined as spin B). Dipolar coupling between spin A and B results in the modulation of the amplitude of the refocused echo (Fig. 4). The modulation frequency is a function of the interspin distance.

DEER has been used to measure distances from 20 to 70 Å in DNA and RNA. Distances in DNA duplexes have been measured using the four-pulse scheme. In 2004, Schiemann *et al.*

measured distances between nitroxides rigidly attached to specific base positions (Table I, entry 4) in a DNA duplex (32). Five distances, ranging from 20 to 55 Å, were measured and were shown to agree very well with values predicted by MD simulations of a standard B-DNA. In 2006, the Qin group used nitroxides attached via the phosphorothioate scheme (Table I, entry 1) to measure distances in a DNA dodecamer and a 68-base-pair duplex (35). Eight distances, ranging from 20 to 40 Å, were measured on the dodecamer (see an example in Fig. 4). The measured distances were found to correlate strongly (R^2 = 0.98) with values calculated using the NMR structure and a conformer search program (Section IV.C). In 2007, Ward *et al.* used nitroxides attached to the 2′-sugar position (Table I, entry 2a) to measure distances in DNA duplexes. Five distances were reported, with the largest distance being 68 Å (83).

Distance measurements in RNA have also been reported. In 2003, Schiemann *et al.* used a three-pulse scheme to measure a distance between nitroxides attached to 2′-sugar positions (Table I, entry 2a) in a RNA duplex (40). This was the first report of SDSL measurements of distances greater than 30 Å in an RNA system. In 2007, distance measurements in RNA duplexes were reported by Schiemann *et al.* using nitroxides rigidly attached to base positions (Table I, entry 4) (34) and by the Qin group using flexible nitroxides attached to the phosphate backbone (Table I, entry 1) (36). These studies found that the measured distances agree very well with those predicted based on either the crystal structure (36) or a standard A-form conformation (34). It was also shown that SDSL measured distances clearly distinguish between A-form duplexes and B-form duplexes (34).

While distance measurements using DEER have been demonstrated in many nucleic acid systems, a number of practical issues are worth noting. The concentrations of the double-labeled sample are generally between 100 and 150 μM (32,34–36,40), although concentrations as low as 25 μM have been used (83). Additionally, in DEER, the lower limit of the measured distance is approximately 15 Å, which is set primarily by the excitation bandwidth requirement (84). The upper limit is approximately 80 Å, and is determined by the phase memory time (T_m) characterizing the dephasing of the electron spin transverse magnetization (84). To achieve a sufficiently long T_m for nanometer distance measurements, samples are measured in a frozen glassy state. In all reported nucleic acid studies, samples were rapidly frozen in liquid nitrogen with glycerol or ethylene glycol added to samples, and EPR measurements were carried out at temperature between 10 and 80 K. Using deuterated solvents can lead to a longer T_m and facilitates long distance measurements (83). Under these experimental conditions, one needs to guard against formation of clusters (e.g., ice crystals), which would negate the assumption of an isotropic distribution of macromolecular orientations (32,35,40,83). Possible interference due to intermolecular spin coupling also needs to be considered (32,35,40,83).

It is also important to consider the procedure for obtaining interspin distances from measured DEER signals, as well as the interpretation of these distances. In studies with rigidly attached nitroxides (Table I, entry 4), the interspin distance distribution is presumably rather narrow, and the interspin distances have been calculated directly from measured Pake patterns (32). However, in most cases, fitting of the DEER signal is required to obtain a distribution, $P(r)$, of the interspin distances. The Tikhonov regularization approach, which does not assume a specific form of $P(r)$, has been the method of choice (85, 86), though options are available for fitting data using model functions such as one or two Gaussians (85). The resulting $P(r)$ may show one population with a narrow width, one population with a broad width, or multiple populations. The interpretation of $P(r)$ is still debated. In a recent study, Ward *et al.* showed that under carefully controlled conditions, a $P(r)$ with features of multiple populations can be analyzed to recover five distance populations that match the five DNA species in the sample (83). In a number of studies, the average distance (35, 36) or the maximum probable distance (34, 83) is used to represent the interspin distance.

C. Interpretation of the Measured Internitroxide Distances, Computational Approaches

Although the distance between the unpaired electrons in a pair of nitroxides can be accurately measured, a challenge in SDSL studies is to correlate the measured internitroxide distances to the three-dimensional structure of the target macromolecule. The unpaired electron in a nitroxide is predominantly localized to the nitroxyl group (15), which is spatially distinct from the site of interest (the nitroxide attachment point). The measured internitroxide distances (r_{NN}, between the two unpaired electrons) are generally different from the actual distances at the parent molecule (r_{target}). The r_{NN}/r_{target} relationship depends on the bonds that link the nitroxide to the target molecule, which varies significantly depending on the nitroxide labeling scheme used (Section III). Furthermore, even if the same nitroxide labeling scheme is considered, the nitroxide conformation may vary significantly between different sites of a folded macromolecule, and the r_{NN}/r_{target} relationship may vary from site to site within the same target molecule. The key issue in correlating r_{NN} and r_{target} is to identify the nitroxide conformers that are allowed at a given labeling site. In SDSL distance measurements in nucleic acid systems, this issue has been adressed using a number of computational approaches, including stepwise conformer searches (35,36,39), molecular dynamics (MD) simulations (24,32,34,39), and simple geometry modeling (83).

1. NASNOX, A Discrete Conformer Search—Haworth *et al.* have developed a program, called NASNOX (35,36,39), that predicts the distances between two R5 nitroxide probes (nitroxides that are attached to DNA or RNA molecules using the phosphorothioate scheme, Table I, entry 1) (Fig. 5). In the NASNOX program, the target macromolecule is input as a pdb file. The target may have an atomic resolution structure that has been experimentally determined by X-ray crystallography or NMR spectroscopy, or it may be a theoretical model generated using computational approaches.

Once a pair of nitroxide labeling sites is specifed at the target molecule, NASNOX models R5 at these sites using experimentally determined bond lengths and bond angles (Fig. 5A) (39). As directed by the user, the R5 probe can be attached to either the R_p, the S_p, or both phosphorothioate diastereomers at a given site. To identify the allowable nitroxide conformers at each labeling site, the program systematically varies the three torsion angles that characterize the rotations of the single bonds linking the pyrroline ring to the nucleic acid (t1, t2, and t3, Fig. 5A). For each nitroxide conformer, defined by a set of t1, t2, and t3, with the nucleic acid coordinates fixed, the program checks for steric collisions between any atom of the nitroxide and any atom of the parent molecule. The conformer without steric collision is recorded as an allowable conformer (Fig. 5B). Once the allowable conformers are identified, the ensemble of inter-R5 distances is computed, and the corresponding mean and standard deviation of the distances are calculated (Fig. 5C).

The NASNOX program has been successfully tested on model DNA and RNA molecules that have atomic resolution structures available (35,36). For inter-R5 distances >20 Å, the mean distances computed by NASNOX agree very well with those measured experimentally (35, 36). The biggest advantage of NASNOX is its speed—each R5 conformer distribution and the corresponding inter-R5 distances can be computed in seconds to minutes on a desktop PC. An internet-accessible version of NASNOX, called NASNOX-W, is available at http://pzqin.usc.edu/NASNOX/ (37).

To ensure the efficiency of the conformer search, NASNOX makes two key assumptions. First, the allowable conformers are determined solely by steric exclusion from DNA, while other forces, such as electrostatic interactions, hydrophobic effects, and hydrogen bonding, are not considered. This assumption is supported by all atom MD simulations of R5-labeled DNA (39) (Section IV.C.2). The second assumption in NASNOX is that the parent molecule coordinates are fixed during the nitroxide conformer search. In the model DNA and RNA

studies, the dynamics of the parent molecule seem to have only minor effects on the average inter-R5 distances, as the values determined by DEER, computed by NASNOX, and predicted by MD agree well with each other (35,36,39). Less-satisfying correlations were found between the NASNOX predicted widths of the distance distributions (the standard deviation of the distribution) and those measured from DEER. This may be due, in part, to dynamics of the parent molecule (35,36,39). Currently, the NASNOX program works only with the R5 label, but the underlying principles should be applicable to other probes.

2. MD Simulations—MD simulations have been used in interpreting measured distances in SDSL studies of nucleic acids (24,32,34,39) and proteins (87). MD simulations account for the physical forces at an atomistic level, and should, in theory, provide a complete description of the behavior of the nitroxide. In practice, in order for a MD simulation to serve as an accurate representation of the behavior of the experimental system, a number of issues need to be addressed. These include the force field (for both the nucleic acid and the nitroxide), the solvent model, and ergodicity (sufficient sampling of the conformational space).

Price *et al.* used MD simulations to examine internitroxide distances between a pair of R5s attached to a DNA dodecamer (39). The simulations used amber98 force field and a full atomistic solvent model. The R5 nitroxide was parameterized based on an empirical approach, and the force field was reported (39). Simulations with different nitroxide starting conformations give convergent results in both the average internitroxide distances and the nitroxide conformer distributions, indicating sufficient sampling of the conformational space. The average distances obtained from the MD simulations agreed with both those determined experimentally by DEER and those predicted using NASNOX. The MD simulations revealed discrete transitions between chemically preferred values (*gauche*$^{+}$, trans, *gauche*$^{-}$) of the torsion angles t1, t2, and t3 (Fig. 5A), as well as steric exclusion between the nitroxide and the DNA. Both of these features are adequately represented in the NASNOX search algorithm, accounting for its success. Simulations also revealed a possible sequence-specific nitroxide–DNA interaction, which was recently confirmed by experiments (Popova and Qin, manuscript in preparation).

Schiemann *et al.* have used MD simulations to interpret distances measured using a class of nitroxides that are linked to a nucleic acid base by an acetylene bond (Table I, entry 4) (32, 34). Their studies used the amber98 force field and an atomistic solvent model. Quantum mechanical calculations based on density functional theory were used to parameterize the nitroxide. The results show a good correlation between the predicted internitroxide distances compared to those measured using DEER (32, 34). For DNA duplexes, it was reported that the B-form structure is maintained in nitroxide-labeled DNA, and that fluctuations in internitroxide distances are largely due to DNA dynamics (32). In the RNA studies, nitroxide-labeled duplexes were found to adopt a nonstandard conformation that is in between the A-form and the B-form, and transient base pair opening in nitroxide-labeled RNA duplexes was detected in the 50-ns trajectories (34).

DeRose *et al.* have carried out short MD simulations on a pair of nitroxides attached to the 2′-positions of RNAs (Table I, entry 2b) (24). Simulations were carried out on idealized A-form RNA duplexes and NMR-derived structures of the TAR RNA. Results were used to interpret cw-EPR measured distances.

Darian and Garnet also reported MD simulations on a single nitroxide that is rigidly attached to base positions of DNA duplexes (88). The reported work includes studies on both five- and six-membered ring nitroxides. The nitroxide was parameterized based on quantum mechanic calculations and crystallographic data. Using data from the MD simulations, the authors

examined the influences of the nitroxide on the DNA structural parameters, such as the helical groove width, helical twist, and displacement of bases.

3. GEOMETRY-BASED Modeling—To interpret distances measured in DNA duplexes, Ward *et al.* modeled the nitroxide as a pseudoatom attached to a simple cylinder that is parameterized based on standard B-form DNA (83). The measured internitroxide distances were fit to the modeled distances by adjusting a set of geometric parameters that describe the positioning of the nitroxide pseudoatom with respect to the DNA and the other nitroxide. A good agreement between the measured and modeled distances was obtained with one set of parameters, suggesting this geometrical model provides a sufficiently accurate representation of nitroxide-labeled DNAs. The geometrical model also agreed with studies that examine the nitroxide pseudoatom in the context of an atomistic model of standard B-form DNA.

D. Distance Measurement Summary

Methods for measuring and interpreting internitroxide distances have now been established. This makes it possible to use SDSL to probe the conformation of a nucleic acid molecule with no known atomic structure. Using a molecular probe, such as a nitroxide, it may not be possible to define an atomic-resolution structure. Instead, internitroxide distances may reveal the global structure of nucleic acids, as defined by the relative spatial orientations between various duplexes within a folded molecule. Work toward this goal is currently underway.

V. Site-Specific Structural and Dynamic Information from a Single-Labeled Nitroxide

CW-EPR spectral analysis is the method most frequently used to obtain information on the local environment of a spin label (2–4,6–9). Both the *g* and *A* tensors of the unpaired electron within the nitroxide are orientation dependent. The cw-EPR spectrum is influenced by the reorientation dynamics of the nitroxide, which average the *g* and *A* tensors. It is possible to analyze the EPR spectrum to obtain information on nitroxide dynamics, and to use this information to better understand features of the local environment.

For a nitroxide covalently attached to a macromolecule, such as a DNA or RNA, the nitroxide dynamics can be thought of as being due to a combination of three types of motions (Fig. 6A). These are the overall rotational motion of the macromolecule (characterized by a rotational correlation time τ_R), the torsional rotation about bonds that connect the nitroxide ring to the macromolecule (τ_i), and the motion of the segment of the macromolecule at or near the labeling point (τ_B) (2). The τ_R motion is uniform at all labeling sites, whereas the τ_i and τ_B motions are specific to the labeling site. The combined effects of τ_R, τ_i, and τ_B determine the observed EPR spectrum. Experimental conditions can be manipulated to enhance spectral effects that are specific to particular mode(s) of motion. For example, site-specific features (τ_i and/or τ_B) can be enhanced by reducing the overall tumbling of the macromolecule, which can be accomplished by increasing solvent viscosity (2,8,9).

In the following sections, we will first discuss methods for characterizing nitroxide dynamics from cw-EPR spectra. Then we will discuss approaches for extracting information about the local environment from the nitroxide dynamics. Specific examples of using cw-EPR to study nucleic acids will then be presented. Our discussions will focus on X-band cw-EPR (~9.5 GHz), as most SDSL studies were carried out at this frequency.

A. Nitroxide Dynamics and EPR Spectral Lineshape

Figure 6B shows simulated X-band EPR spectra of nitroxides undergoing isotropic tumbling. Three regimes can be defined by the sensitivity of the EPR spectral lineshape to the nitroxide

dynamics, which are characterized by an overall rotational correlation time τ. The fast motion limit corresponds to $\tau \sim 10^{-11} - 10^{-9}$ s (4, 11, 17). In this regime, only the isotropic average of the magnetic interactions will be observed. The spectrum shows three sharp lines because of nearly complete averaging of the *g* and *A* tensors (Fig. 6B, τ = 0.1 ns), and the peak heights and peak widths of the spectrum are sufficient to characterize the nitroxide motion (4, 8, 11, 17, 89).

In the rigid limit ($\tau > 3 \times 10^{-8}$ s at X-band), a static distribution of all possible nitroxide orientations is present, and the cw-EPR spectrum is the sum of lineshapes from all possible values of the *g* and *A* tensors (a powder spectrum). The splitting between the outermost peaks (2A) is readily measured (Fig. 6B) and can be used as an empirical parameter to characterize the nitroxide dynamics (4,8,11,17,89).

In the slow-motion regime (1×10^{-9} s < τ < 3×10^{-8} s), *g* and *A* tensor averaging is incomplete. The cw-EPR spectrum is most sensitive to nitroxide rotation, and drastic lineshape changes can be observed depending on nitroxide motions. As the nitroxide motion decreases (τ increases), the central line becomes broader, new features become apparent at the low-field and the high-field regions, and splitting between the outer peaks increases (Fig. 6B). It should be noted that as the EPR frequency changes, the time domain in which spectral variations are observed also changes.

In the slow-motion regime, quantitative spectral analysis is much more challenging. Given a particular physical model of nitroxide dynamics, one can compute the EPR spectrum. However, given an experimentally observed EPR spectrum, it is difficult to obtain a quantitative and unambiguous description of the nitroxide dynamics. A number of approaches, with varying levels of precision, have been used to characterize nitroxide dynamics from a given EPR spectrum. These will be discussed in the following section.

B. Characterizing Nitroxide Dynamics at the Slow-Motion Regime

1. Semiempirical Approaches—Many SDSL studies have used a semiquantitative approach to spectral analysis, in which simple parameters measured directly from the EPR spectrum are used to characterize the nitroxide dynamics (3). These parameters include the width of the central line (ΔH_{pp},Fig. 6B), the splitting of the resolved hyperfine extrema (2A, Fig. 6B), and the second moment of the spectrum ($\langle H_2 \rangle$, characterizing how broad the spectrum is) (90). These parameters report on the nitroxide mobility describing a combined effect of the rate and the amplitude of motion. For example, a broad center line gives a small $(\Delta H_{pp})^{-1}$ value and indicates low mobility, which can result from low frequency but large amplitude motions, or small amplitude motions with fast rates.

Although the lineshape parameters do not directly give the rate and amplitude of motion, they provide a means to quickly access relative nitroxide mobility at different sites. The semiempirical nitroxide mobility characterization approach has been widely used in protein studies (2,3,6,91). It has also been shown to be capable of qualitatively capturing structural and dynamic features of nucleic acids at the level of individual nucleotides (9), and has been used to probe nucleic acid structures and to monitor conformational changes (Sections V.D.3 to V.D.5).

2. Spectral Simulations in the Slow-Motion Regime—Two approaches have been used to simulate EPR spectra in the slow-motion regime. One approach uses MD to simulate the time-dependent trajectories of axes that are fixed with respect to the nitroxide (the nitroxide frame), and uses these trajectories to calculate the EPR spectrum directly (92–94,134–137). However, this approach is very demanding in terms of computational resources, and its success depends on generating trajectories that sufficiently sample the free energy landscape (95). The

trajectory-based approach has not been widely used in conjunction with nucleic acid SDSL, although this may change with advances in computer speed and simulations techniques.

A more widely used approach in EPR spectral simulation is based on the stochastic Liouville equation (SLE) (96). In the SLE, the electronic and nuclear spins are treated quantum mechanically, whereas the nitroxide reorientation motion is treated classically and parameterized in terms of rotational diffusion constants. The SLE approach is extremely efficient and capable of computing a spectrum in a fraction of a second. This enables iterative fitting of experimental spectra.

Two SLE-based simulation approaches have been developed in studies of nitroxides attached to bases within DNA duplexes (25,97). The Bobst group developed a base disk model, in which the spin-labeled base is considered an axially symmetric diffusing system (25,29). The principle motion is characterized by two correlation times: $\tau_{\parallel}$ describes rotational diffusion about the principle axis as defined by the average position of the bonds that connect the base to the nitroxide, and $\tau_{\perp}$ describes the motion about the axis perpendicular to the tether bond. $\tau_{\perp}$ is used to characterize motions of the labeled base, which includes contributions from DNA global tumbling, the collective bending and twisting of the DNA segment, and twisting/tilting of the individual base.

Robinson *et al.* used a SLE-based approach to simulate spectra of nitroxides that are rigidly tethered to bases within a DNA duplex (97). In this approach, the DNA helix is treated as a cylinder with internal motion. The overall tumbling of the DNA duplex is treated explicitly according to hydrodynamic models. All the internal motions are treated in the fast motion limit, and their collective effects are accounted for using motionally averaged effective g and A tensors. Spectra are simulated using a single parameter, the mean-square oscillation amplitude of the nitroxide attached to the ith base pair. The mean-square oscillation amplitude is directly related to the order parameter, but the simulation does not produce any estimation of the correlation time for the internal dynamics. For nitroxides that are more flexibly attached to bases within a DNA duplex (e.g., Table I, entry 5), the Bobst group has taken a similar approach and developed a dynamic cylinder model (29), which yields an order parameter that describes the amplitude of the nitroxide motion. It was suggested that the order parameter reports on both the base dynamics and the motion of the nitroxide with respect to the base.

Simulation models used in DNA duplex studies described above can be regarded as special cases in a family of SLE-based EPR simulation programs developed in the Freed group (98–100). These programs describe the diffusive motion of the nitroxide under the constraint of an orienting potential. The orienting potential is expressed as a function of the polar angles of a director axis in a rotational diffusion frame, and yields an order parameter (S) for the motion being described. In each system, the rotational diffusion frame is fixed with respect to the structure of the nitroxide, although its exact orientation may vary from system to system. Similarly, the director is fixed at the target macromolecule, such as the helical axis of a DNA duplex (101), in a system-dependent fashion. Simulations provide both a rate (τ) and an order parameter (S) to describe the partially ordered (restrictive) diffusive motion of the nitroxide with respect to the target macromolecule.

One of the programs developed by the Freed group is called the *m*icroscopic *o*rdered *m*acroscopic *d*isordered (MOMD) model (99). In MOMD simulations, the spin label undergoes microscopic molecular ordering with respect to a local director, which is a frame fixed at the target macromolecule. The local directors (the macromolecule themselves), however, are oriented randomly and rigidly fixed with respect to the laboratory frame (generally defined by the applied magnetic field). The resulting EPR spectrum is obtained by integrating over the distribution of the local director orientations. The MOMD program is most useful in crystalline

and liquid crystalline systems, but may also be used to describe systems where the global tumbling of the macromolecule is slow with respect to the EPR timescale. The MOMD approach has been used to simulate SDSL spectra in RNA (31,102) and DNA (101).

Another program developed by the Freed group is called the *slowly relaxing local structure* (SRLS) model (100). In SRLS simulations, the orienting potential itself is allowed to undergo rotational diffusive motion on the EPR timescale. The model describes the situation where the spin label is reorienting with respect to the parent macromolecule, whereas the macromolecule is slowly tumbling. This model has been applied to DNA duplexes (101).

In MOMD and SRLS simulations, some of the parameters such as the *g* and *A* tensors are independently determined. However, it is well known that certain parameters in the simulation are correlated and not uniquely determined. For example, within a certain range, S and τ may covary (99,103). When such correlations are identified, allowable ranges of each parameter are determined by exploration of the parameter space to estimate probable uncertainties. In protein studies, it has been demonstrated that a global fitting of EPR spectra at multiple frequencies may provide better constraints for the parameters (100).

One may also constrain the simulation parameters by simultaneously analyzing a group of spectra measured using chemically modified nitroxides. For example, in studies of protein (103) and RNA (31), simultaneous analyses have been carried out on spectra obtained from nitroxides that are modified at the 4-position of the pyrroline ring. These modifications systematically introduce larger functional groups (i.e., 4-H, 4-CH_3, 4-Br, and 4-phenol), and are expected to increasingly restrict rotations about the bonds that connect the pyrroline ring to the parent macromolecule. In the spectral simulations, such effects are accounted for by increasing the order parameter while keeping the rate of nitroxide motion fixed (31,103).

C. Correlating Nitroxide Motion to Local Structural and Dynamic Features

Methods described in Section V.B allow one to characterize nitroxide motion with varying levels of precision. The challenge for SDSL lies in the determination of local environmental feature(s) that give rise to the observed nitroxide motion (or EPR spectrum).

1. Probing the Local Environment Using Semiempirical Nitroxide Mobility—

Many studies have demonstrated qualitative correlations between features at the labeling site and the nitroxide mobility as characterized by the semiquantitative approach (Section V.B.1) (2,3,6–9). In nucleic acid SDSL, a high-mobility nitroxide generally reports a highly flexible labeling site, such as unpaired and unstacked nucleotides in single strand or loop regions (23, 31). A low-mobility nitroxide generally reveals structural and/or dynamic constraints at the labeling site, such as stacking and/or hydrogen-bonding (23,31,102), as well as tertiary contacts within a folded RNA (44).

In RNA SDSL studies using a nitroxide attached at a modified uridine base (Table I, entry 3a), Qin *et al.* have reported that different secondary structures (e.g., single-strand, stacked A/U pair, and U/U mismatch) give clearly distinct lineshapes, whereas the stacked A/U pair spectrum gives a very similar lineshape in two different RNA molecules (102). This has led to the proposal of building a library in which observed spectral lineshapes are categorized based on known RNA structures (102). The library will reveal both spectral *divergence* (distinctive lineshapes for different elements) and spectral *convergence* (similar lineshapes for the same element in different contexts). If successful, the library will enable lineshape-based structure identification at any RNA site.

In protein SDSL studies, semiquantitative mobility analysis is frequently coupled with nitroxide scanning (2). In this approach, nitroxide mobility is measured, one residue at a time,

along a stretch of amino acid sequence, and the periodicity in the nitroxide mobility variation experimentally identifies the secondary structural element (e.g., 3.6 residue/period for the α-helix). However, similar nitroxide scanning experiments have not been reported in studies of nucleic acids. This may be due to the difficulty in scanning the nitroxide along a given nucleic acid sequence using most of the available nitroxide labeling methods. Recent data suggest that nitroxides attached using the phosphorothioate labeling scheme (Table I, entry 1) can be used to monitor the local environment at the level of individual nucleotides (Popova and Qin, manuscript in preparation). This nitroxide label may be a good candidate for scanning nucleic acids. Additionally, secondary structural elements in nucleic acids generally involve a much more extended segment of the primary sequence (e.g., ~10 base pairs per turn in A or B-form duplexes). Further studies are needed to determine what kind of information can be obtained from nitroxide scanning in nucleic acids.

2. Probing the Local Environment with Quantitative Spectral Simulations— Spectral simulations yield a set of quantitative parameters based on a given model. The simulated parameters define the correlation between the nitroxide motion and the features of the parent molecule. In each simulation, assumptions have to be made regarding what type of motions (parameters) are tractable and how these motions are related to the structural and dynamic features of the parent macromolecule. These assumptions need to be tested experimentally.

One approach for correlating parameters obtained from spectral simulations to local structural features is to carry out systematic molecular level mutations, either at the macromolecule or at the nitroxide probe, and to evaluate their effects on the simulation parameters (11,14). For example, in studies of nitroxides attached to bases within DNA duplexes, the Robinson group explicitly accounts for the DNA duplex global tumbling, and extracts a parameter equivalent to the mean-square oscillation amplitude of the spin-labeled base pair (Section V.B.2) (97, 104). Studies were then carried out with varying DNA lengths, sequences, and nitroxide labeling positions. Effects of these changes on the mean-square oscillation amplitude were used to test assumptions made in the spectral simulation (104). Once validated, the mean-square oscillation amplitude was used to extract information on length-independent segmental deformation in DNA duplexes (104–106).

As noted in work from both the Bobst and Robinson groups (11,14), nitroxide motions can be influenced by a wide variety of factors that may change between systems as well as between different chemical labeling schemes. Quantitative correlation of the observed EPR lineshape to local structural and dynamic features remains a challenging task. Advances on this front will likely require a combination of theoretical and experimental efforts.

D. Examples of Application

Selected cases from the literature are presented in this section to illustrate methods discussed in Sections VA–V.C. In Section V.D.1, we will discuss the use of measuring the global tumbling of the nitroxide-labeled macromolecules to monitor molecular interactions. Then we will discuss examples of EPR lineshape analysis and their applications in probing site-specific features in DNA duplexes (Section V.D.2) and folded RNA molecules (Sections V.D.3–V.D.5). Currently, we are aware of few reported examples on using nitroxide-labeled nucleic acids to investigate protein–nucleic acid interactions (11). With the advances in SDSL, protein–nucleic acids interactions present an interesting area for future exploration.

1. Monitoring Molecular Interactions via the τ_R Effect—The τ_R effect refers to a change in the EPR lineshape due to a change in the overall tumbling of the macromolecule. A simple estimation based on the molecular weight of a 25-nt oligonucleotide (~7500 Da) gives

an overall tumbling rate τ_R of approximately 4 ns in aqueous solution at room temperature (31,107). One expects that tumbling of this short oligonucleotide affects the X-band EPR spectrum. Interactions between such an oligonucleotide and other macromolecules, such as a complimentary strand (11), a partner nucleic acid (22), or a protein (11), increase the molecular weight of the system. This leads to changes in the overall tumbling of the complex, which are reflected in the nitroxide lineshape.

The τ_R effect has been used to detect nucleic acid hybridizations (11). In the 1970s, Bobst *et al.* used spin-labeled polyU to detect the polyA tract in mRNAs (10). More recently, Gannet *et al.* reported detection of DNA triplex formation using spin-labeled oligonucleotides (30). In these studies, hybridization of a nitroxide-labeled oligonucleotide to its complimentary strand leads to a drastic reduction of the overall tumbling rate, which is reflected as line broadening in the EPR spectrum. The change of EPR lineshape is due to a combined τ_R and τ_i/τ_B effects, as hybridization reduces the overall tumbling of the oligonucleotide as well as motions of the nitroxide-labeled nucleotide(s) due to hydrogen bonding and stacking. Recently, Bobst *et al.* reported a reverse approach to detect DNA hybridization, in which a single genome is identified by monitoring the appearance of fast-tumbling fragments (108).

Qin *et al.* used the τ_R effect to study a frequently used RNA tertiary interaction motif—binding between a GAAA tetraloop and its RNA receptor (22) (Fig. 7). Upon binding of an RNA hairpin containing the GAAA tetraloop to its RNA receptor, increases in the molecular weight of the complex gave rise to EPR spectral broadening (Fig. 7). The dissociation constant (K_d) was measured to be 0.4 mM between the GAAA tetraloop and its receptor, which is a weak interaction and is difficult to measure using other methods (22). This study illustrates several facets of using the τ_R effect to monitor interactions in nucleic acids. First, the nitroxide is attached far away from the interface between the tetraloop and the receptor (Fig. 7A), allowing one to monitor the interaction with minimal perturbation. Second, as the spin label concentration in an EPR experiment is generally >10 μM, the method is suitable for measuring interactions where the K_d is approximately 10–1000 μM. Third, the EPR measurements can be carried out with a wide range of buffer conditions.

2. Dynamic Behavior of DNA Duplexes—The Bobst group studied a large number of double-stranded DNAs and RNAs using thymidylates and deoxycytidylates that are substituted at position 5 with nitroxides containing tethers ranging from 2 to 11 atoms (Table I, entry 5) (11). Data on B-form DNA duplexes were simulated using a model that characterizes nitroxide motions by two correlation times, $\tau_{\parallel}$ and $\tau_{\perp}$ (Section V.B.2) (25, 29, 101, 109). $\tau_{\parallel}$ was found to be tether dependent, was less than 1 ns, and was attributable to nitroxide motion that was independent of base motion (11). $\tau_{\perp}$ was thought to represent motions including twisting and tilting of the individual base, collective bending and twisting of the DNA segment, and global tumbling of DNA (25, 29, 101, 109). Values of $\tau_{\perp}$ from all double-stranded systems were reported to be in the 1–10 ns range (11, 25, 29, 101, 109), leading to the conclusion that there are significant base motions and these motions contribute to the dynamics of the nitroxide. However, questions have been raised as to the degree to which $\tau_{\perp}$ is influenced by the motion of the tether versus that of the base (see below) (14).

The Robinson group used nitroxides that are rigidly coupled to a DNA base (T^* and dQ, Table I, entry 4a and entry 6a) to examine dynamics in B-form DNA duplexes (14, 97, 104–106, 110). A mean-square oscillation amplitude, obtained by simulating the observed EPR spectra, was used to obtain information on the DNA (Section V.B.2) (97). The authors concluded that the global tumbling of the DNA duplex is accurately described by hydrodynamic theory (97), and the internal collective DNA deformation fits well to a modified weakly bending rod model (104). The observed spectra also depend on sequence variations that are distant from the label, and efforts have been made to account for these observations using a sequence-dependent force

bending constant (105, 106). Furthermore, the Robinson group reported that DNA duplex flexibility is linked to phosphate backbone neutralization (110).

From studies with rigidly tethered nitroxide probes, Robinson *et al.* concluded that there are no large amplitude fluctuations of the labeled base (14), which contradicts conclusions drawn from studies using flexible nitroxides (11). There has been debate over whether the rigidly coupled nitroxides alter the behavior of the base, and if so, to what degree (11,14,29,101, 109). On the other hand, for the flexible nitroxides, questions have been raised regarding whether motions of the flexible linker lead to an overestimation of base dynamics (14). Furthermore, Bobst *et al.* have reported that the short-tether nitroxide may give rise to a multiple component spectrum (101), which may further complicate quantitative analysis. These studies illustrate an important issue in SDSL. The information one can gain from the nitroxide depends on how strongly the nitroxide is coupled to the target molecule, and therefore the tether plays a very significant role. An ideal tether would completely couple the nitroxide to the base, yet would not at all alter its behavior. In practice, such a tether may not ever be developed.

Other studies have examined base mismatches and bulges in DNA duplexes (11,111). The results generally show distinct nitroxide lineshape changes indicating variation in nitroxide dynamics. However, quantitative interpretations have not been reported.

3. The TLR RNA—Qin *et al.* have reported SDSL studies on a 23-nt RNA, designated as TLR, that contains two structural elements—the UUCG loop and the 11-nt motif of the GAAA tetraloop receptor (31). Three nitroxide variants were attached, one at a time, to six uridine positions within the TLR molecule using the 4-thioU scheme (Table I, entry 3a). The observed lineshapes vary significantly among the different uridine sites, which is consistent with the expected versatility in RNA structures. For example, at the $U_{11}U_{12}CG$ loop, mobility parameters obtained by semiquantitative analysis showed that the nitroxide at U11 has low mobility, whereas that at U12 is highly mobile (Fig. 8) (31). This is consistent with NMR studies showing that U11 is hydrogen-bonded and stacked, and U12 is structurally unrestrained and highly dynamic (112,113). This suggests that the nitroxide is reporting RNA base motion.

MOMD simulations were carried out for spectra obtained at U16, which participates in a Watson-Crick base pairing interaction (Fig. 9) (31). The analyses led to a proposed motion model for nitroxides attached via the 4-thioU scheme, where in the absence of RNA–nitroxide interaction, rotations about the distal two bonds (the X_3^r X_4^r torsion angles, Fig. 9) are the major contributors to the EPR spectrum. The characteristic lineshape at U16 was observed at a stacked Watson-Crick A/U base pair in another RNA molecule, a dodecameric RNA duplex (102), suggesting that this motion model may be general. The U16 lineshape is also the first experimental evidence of spectral convergence, where the same secondary structure elements embedded in different molecules give the same characteristic lineshape (102).

The nitroxide-labeled TLR molecules allowed the detection of conformational changes in the GAAA tetraloop receptor upon tetraloop docking (114). Increases in nitroxide mobility were observed at U19 upon formation of the tetraloop/receptor complex (Fig. 10), and experiments linked the nitroxide mobility increase to increases in the dynamics of the U19 base (114). This suggests that U19 becomes unstacked in the complex, which is consistent with the crystal structure showing that U19 flipped out of the helix as the tetraloop docks (Fig. 10) (115).

4. HIV trans-Activation Responsive RNA—The *trans*-activation responsive (TAR) RNA is the 5′-leader sequence of the HIV-1 mRNA genome. Interaction between the TAR RNA and the Tat protein is a key determinant in viral transcription, and the Tat/Tat complex has long been a target for therapeutic intervention of HIV replication (116). Sigurdsson *et al.* have attached nitroxides to the 2′-sugar position (Table I, entry 2a) of four specific uridine

nucleotides within a 27-nt RNA construct that contains the TAR element (23) (Fig. 11). In the TAR RNA alone, nitroxides attached at the two base-paired sites were found to report the overall tumbling of the TAR RNA, while those at the bulge region showed significantly higher mobility, similar to that of a single strand (23). These studies established that the nitroxide attached at the 2′ -sugar position is capable of reporting site-specific features of the RNA local environment at the level of a nucleotide.

Using the spin-labeled TAR RNAs, Sigurdsson *et al.* carried out extensive studies on local structural and dynamic changes in HIV TAR that are induced by interactions with ligands, including small molecules (42), metal ions (41,43), and peptides (41,117). In these studies, the semiquantitative mobility parameters are used to characterize the nitroxide spectra in the presence and absence of the ligand. A dynamic signature for each ligand is determined based on the pattern of nitroxide mobility changes as a function of nucleotide position. This is used as a qualitative but effective means to characterize the RNA response to various ligands. Figure 11 shows an example of dynamic signatures observed from complexes between TAR RNA and small molecules (42). The data indicated that ligands that are known to bind similarly to the TAR RNA give nearly identical patterns, whereas ligands that bind at different sites give clearly different patterns (Fig. 11). The dynamic signature was used in conjunction with other information to understand TAR-small molecule interactions.

5. Hammerhead Ribozyme—The hammerhead ribozyme is a small self-cleaving RNA motif that catalyzes a transesterification reaction at a specific site. It has been a model system for understanding RNA catalysis, structure and folding, conformational dynamics, and metal ion interaction (118). The DeRose group used SDSL to probe metal ion interactions in an extended hammerhead construct, in which an extended loop–loop interaction enhanced catalytic activity (44). Nitroxides were attached to 2′-sugar positions (Table I, entry 2b) of specific uridine and cytosine sites. Changes in the observed nitroxide lineshape at a specific site (U1.6) were assigned to tertiary contacts arising from interactions between the extended loops upon RNA folding. By analyzing the observed U1.6 spectra, it was found that this RNA folding event occurs at a much lower Mg^{2+} concentration compared to what is required for enhanced catalytic activity.

The Sigurdsson group used SDSL to study RNA dynamics in a truncated hammerhead (45). The nitroxide was attached to a uridine near the catalytic core. EPR was used to monitor variations in RNA conformations in response to metal ions, ribozyme inhibitors, and pH changes. The data indicate a two-step metal ion-dependent folding pathway, which is consistent with previous studies using other biophysical and biochemical techniques.

VI. Beyond Distance Measurements and Nitroxide Dynamics Analysis

In addition to nitroxide dynamics analysis and distance measurements, a number of additional EPR measurements have been used in SDSL studies of protein and membrane systems (2,4, 8). We briefly describe some of these measurements in this section. Although these measurements have not been widely used in SDSL studies of nucleic acids, they should provide exciting opportunities for future investigations.

A. Nitroxide-Solvent Accessibility

The solvent accessibility of nitroxides has been used extensively to map protein secondary structures, to reveal the global topology of proteins, and to orient proteins with respect to their environments (e.g., lipid bilayers) (2,4,8). Collisions between a nitroxide and paramagnetic agents (e.g., oxygen, metal ion complexes, or other nitroxides) give rise to additional nitroxide relaxation pathways. By measuring these relaxation effects using either cw-EPR or pulsed EPR techniques, one can obtain information on the collision frequency between the nitroxide and

the paramagnetic agent in solution, which is directly correlated to the solvent accessibility at the nitroxide.

There are few reports of measuring nitroxide-solvent accessibility in nucleic acids systems. Shin and Hubbell used nitroxide accessibility to study electrostatic potential distributions around a DNA duplex (119). In the study, a DNA duplex was randomly intercalated by a nitroxide-modified acridine. Collision rates were measured between the nitroxide and neutral and charged paramagnetic agents. The ratio between the collision rates allows one to calculate the average electrostatic potential sensed by the nitroxide. The study found that the electrostatic potential distribution around a DNA duplex agrees with that predicted by the nonlinear Poisson–Boltzmann model. In addition, Robinson *et al.* used pulsed EPR to measure the T_1 relaxation rate of nitroxides attached to DNA duplexes, and examined how the measured T_1 is affected by oxygen in the solution (120).

B. Polarity Effects

The polarity of the environment at the nitroxide tunes the localization of the unpaired electron within the nitroxyl group of the nitroxide, giving rise to changes in the *A* and *g* tensor. This enables one to use the nitroxide as a probe for local polarity, pH, and the formation of hydrogen bonds with the nitroxyl group (17). This effect has been used extensively in studies of membranes and proteins (17,121). Currently, we are not aware of reports on polarity measurements in nucleic acid SDSL.

C. Paramagnetic Relaxation Enhancement

PRE refers to an increase in the relaxation rate of nuclear magnetization due to magnetic dipolar interaction between a nucleus (e.g., ^{1}H) and an unpaired electron. Because the magnetic moment of the unpaired electron is large, PRE can be effective over long distances, extending in the case of Mn^{2+}, for example, up to ~35 Å [see a recent review by Clore *et al.* (122)].

Nitroxides have been shown to be suitable for PRE measurements in studies of proteins and protein/nucleic acid complexes. For example, Varani *et al.* have reported PRE measurements in the structural determination of a protein/RNA complex. The study places a nitroxide at a modified uridine position (Table I, entry 3b) in an RNA hairpin. PRE was measured between the labeled RNA and a double-stranded RNA-binding domain (dsRBD) of the *Staufen* protein from *Drasophila*.(46–48). The measurements provided long-range distance constraints (up to ~15 Å) between the RNA and the protein, which aided in structural determination of the complex. More recently, PRE using nitroxide-labeled RNA was also reported in studies of the dsRBD of Rnt1p RNase III (123). Furthermore, nitroxides attached to proteins have been used to investigate the U1A protein/PIE RNA complex (49).

Recent work from the Clore group has used EDTA-Mn^{2+} complex as the paramagnetic probe to study low population encounter complexes in protein–DNA recognition, as well as large-scale dynamics in nonspecific protein–DNA interactions (122). In studies of RNA and protein/RNA complexes, divalent metal ions such as Mn^{2+} may be potentially involved in RNA folding and function (see Section VI.D), and the nitroxide spin label may provide an alternative probe for PRE.

D. Probing Paramagnetic Metal Ions in RNA Folding and Function

Because DNA and RNA are highly negatively charged polymers, metal ions, such as Na^+, K^+, and Mg^{2+}, play important roles in the structure and function of nucleic acids. For example, it is well known that Mg^{2+} plays critical roles in the folding and catalysis of ribozymes (124). The paramagnetic Mn^{2+} ion, similar to Mg^{2+} in ionic radius and enthalpy of hydration, is capable of supporting functions of many ribozymes and has been utilized as an EPR probe for

studying Mg^{2+}–RNA interactions (124). Studies have been carried out onnucleotides (125) aswell as large-structured RNAs, including the hammerhead ribozyme and tRNA (126–132). A variety of EPR techniques, such as cw-EPR, ENDOR (electron nuclear double resonance), and ESEEM (electron spin echo envelope modulation), have been used to obtain information on metal-binding sites, including locations, number of metal ions bound, affinity, ligand identity, and site geometry (125–132).

VII. Future Directions

SDSL studies of nucleic acids provide unique structural and dynamics information that compliments results obtained using other biophysical techniques. Advances in EPR spectroscopy and nitroxide labeling will make it possible to explore a number of important questions in the future. These include, but are not limited to, mapping global structures of nucleic acids and protein/nucleic acid complexes, monitoring dynamics in large nucleic acid assemblies, investigating site-specific electrostatic features, and investigating metal ion interactions.

Acknowledgments

We thank Gian G. Grant, Anna Popova, and Maria Frushicheva for advice and assistance in preparing the manuscript. Financial support is provided by the National Institutes of Health (R01 GM069557) and the National Science Foundation (MCB0546529). The authors also thank the William R. Wiley Environmental Molecular Sciences Laboratory for a pulse EPR instrumentation time award.

References

1. Altenbach C, Flitsch SL, Khorana HG, Hubbell WL. Structural studies on transmembrane proteins. 2. Spin labeling of bacteriorhodopsin mutants at unique cysteines. Biochem 1989;28:7806–7812. [PubMed: 2558712]
2. Hubbell WL, Altenbach C. Investigation of structure and dynamics in membrane proteins using site-directed spin labeling. Curr Opin Struct Biol 1994;4:566–573.
3. Hubbell WL, Cafiso DS, Altenbach C. Identifying conformational changes with site-directed spin labeling. Nat Struct Biol 2000;7:735–739. [PubMed: 10966640]
4. Fajer, PG. Electron spin resonance spectroscopy labeling in proteins and peptides analysis. In: Meyers, R., editor. Encyclopedia of Analytical Chemistry. John Wiley & Sons; Chichester: 2000. p. 5725-5761.
5. Borbat PP, Costa-Filho AJ, Earle KA, Moscicki JK, Freed JH. Electron spin resonance in studies of membranes and proteins. Science 2001;291:266–269. [PubMed: 11253218]
6. Columbus L, Hubbell WL. A new spin on protein dynamics. Trends Biochem Sci 2002;27:288–295. [PubMed: 12069788]
7. Fanucci GE, Cafiso DS. Recent advances and applications of site-directed spin labeling. Curr Opin Struct Biol 2006;16:644–653. [PubMed: 16949813]
8. Klug CS, Feix JB. Methods and applicants of site-directed spin labeling EPR spectroscopy. Methods Cell Biol 2008;84:617–658. [PubMed: 17964945]
9. Qin PZ, Dieckmann T. Application of NMR and EPR methods to the study of RNA. Curr Opin Struct Biol 2004;14:350–359. [PubMed: 15193316]
10. Bobst AM, Sinha TK, Pan YCE. Electron spin resonance for detecting polyadenylate tracts in RNAs. Science 1975;188:153–155. [PubMed: 163495]
11. Keyes, RS.; Bobst, AM. Spin-labeled nucleic acids. In: Berliner, LJ., editor. Biological Magnetic Resonance. Plenum Press; New York: 1998. p. 283-338.
12. Bondarev GN, Isaev-Ivanov VV, Isaeva-Ivanova LS, Kirillov SV, Kleiner AR, Lepekhin AF, Odinzov VB, Fomichev VN. Study on conformational states of *Escherichia coli* tRNAPhe in solution by a modulation-free ESR-spectrometer. Nucleic Acids Res 1982;10:1113–1126. [PubMed: 6278435]

13. Nothig-Laslo V, Zivkovic T, Kucan Z, Weygand-Durasevic I. Binding of spermine to tRNATyr stabilizes the conformation of the anticodon loop and creates strong binding sites for divalent canons. Eur J Biochem 1981;117:263–267. [PubMed: 6268406]
14. Robinson BH, Mailer C, Drobny G. Site-specific dynamics in DNA: Experiments. Annu Rev Biophys Biomol Struct 1997;26:629–658. [PubMed: 9241432]
15. Makinen, MW.; Mustafi, D.; Kasa, S. ENDOR of spin labels for structure determination: From small molecules to enzyme reaction intermediates. In: Berliner, LJ., editor. Biological Magnetic Resonance. Springer-Verlag, New York, LLC; 1998. p. 181-249.
16. Berliner, LJ. Spin Labeling: Theory and Applications. Academic Press; New York: 1976. p. 592
17. Marsh D. Electron spin resonance: Spin labels. Mol Biol Biochem Biophys 1981;31:51–142. [PubMed: 6262623]
18. Eaton, GR.; Eaton, SS.; Berliner, LJ. Biol Mag Res Vol. Vol. 19. Kluwer; New York, NY: 2000. Distance Measurements in Biological Systems by EPR.
19. Pake GE. Nuclear resonance absorption in hydrated crystals: Fine structure of the proton Line. J Chem Phys 1948;16:327–336.
20. Caruthers, MH.; Beaton, G.; Wu, JV.; Wiesler, W. Chemical synthesis of deoxyoligonucleotides and deoxyoligonucleotide analogs. In: Lilley, DMJ.; Dahlberg, JE., editors. Method Enzymol. Elsevier Science& Technology Books, Academic Press Inc.; San Diego: 1992. p. 3-20.
21. Usman N, Cedergren R. Exploiting the chemical synthesis of RNA. Trends Biochem Sci 1992;17(9): 334–339. [PubMed: 1384179]
22. Qin PZ, Butcher SE, Feigon J, Hubbell WL. Quantitative analysis of the GAAA tetraloop/receptor interaction in solution: A site-directed spin labeling study. Biochem 2001;40:6929–6936. [PubMed: 11389608]
23. Edwards TE, Okonogi TM, Robinson BH, Sigurdsson ST. Site-specific incorporation of nitroxide spin-labels into internal sites of the TAR RNA. Structure-dependent dynamics of RNA by EPR spectroscopy. J Am Chem Soc 2001;123:1527–1528. [PubMed: 11456739]
24. Kim N, Murali A, DeRose VJ. A distance ruler for RNA using EPR and site-directed spin labeling. Chem Biol 2004;11:939–948. [PubMed: 15271352]
25. Kao SC, Polnaszek CF, Toppin CR, Bobst AM. Internal motions in ribonucleic acid duplexes as determined by electron spin resonance with site-specifically spin-labeled uridines. Biochem 1983;22:5563–5568.
26. Kao SC, Bobst AM. Local base dynamics and local structural features in RNA and DNA duplexes. Biochem 1985;24:5465–5469. [PubMed: 2416342]
27. Spaltenstein A, Robinson BH, Hopkins PB. A rigid and nonperturbing probe for duplex DNA motion. J Am Chem Soc 1988;110(4):1299–1301.
28. Miller TR, Alley SC, Reese AW, Solomon MS, McCallister WV, Mailer C, Robinson BH, Hopkins PB. A probe for sequence-dependent nucleic acid dynamics. J Am Chem Soc 1995;117(36):9377–9378.
29. Keyes RS, Bobst AM. Detection of internal and overall dynamics of a two-atom-tethered spin-labeled DNA. Biochem 1995;34:9265–9276. [PubMed: 7619828]
30. Gannett PM, Darian E, Powell J, Johnson EM, Mundoma C, Greenbaum NL, Ramsey CM, Dalal NS, Budil DE. Probing triplex formation by EPR spectroscopy using a newly synthesized spin label for oligonucleotides. Nucleic Acids Res 2002;30:5328–5337. [PubMed: 12466559]
31. Qin PZ, Hideg K, Feigon J, Hubbell WL. Monitoring RNA base structure and dynamics using site-directed spin labeling. Biochem 2003;42:6772–6783. [PubMed: 12779332]
32. Schiemann O, Piton N, Mu Y, Stock G, Engels JW, Prisner TF. A PELDOR based nanometer distance ruler for oligonucleotides. J Am Chem Soc 2004;126:5722–5729. [PubMed: 15125665]
33. Barhate N, Cekan P, Massey AP, Sigurdsson S Th. A nucleoside that contains a rigid nitroxide spin label: A fluorophore in disguise. Angew Chem Int Ed 2007;46(15):2655–2658.
34. Piton N, Mu Y, Stock G, Prisner TF, Schiemann O, Engels JW. Base-specific spin-labeling of RNA for structure determination. Nucleic Acids Res 2007;35(9):3128–3143. [PubMed: 17452362]
35. Cai Q, Kusnetzow AK, Hubbell WL, Haworth IS, Gacho GP, Van Eps N, Hideg K, Chambers EJ, Qin PZ. Site-directed spin labeling measurements of nanometer distances in nucleic acids using a

sequence-independent nitroxide probe. Nucleic Acids Res 2006;34:4722–4734. [PubMed: 16966338]

36. Cai Q, Kusnetzow AK, Hideg K, Price EA, Haworth IS, Qin PZ. Nanometer distance measurements in RNA using site-directed spin labeling. Biophys J 2007;93(6):2110–2117. [PubMed: 17526583]
37. Qin PZ, Haworth IS, Cai Q, Kusnetzow AK, Grant GPG, Price EA, Sowa GZ, Popova A, Herreros B, He H. Measuring nanometer distances in nucleic acids using a sequence-independent nitroxide probe. Nat Protoc 2007;2(10):2354–2365. [PubMed: 17947978]
38. Nagahara S, Murakami A, Makino K. Spin-labeled oligonucleotides site specifically labeled at the internucleotide linkage. Separation of stereoisomeric probes and EPR spectroscopical detection of hybrid formation in solution. Nucleosides Nucleotides 1992;11:889–901.
39. Price EA, Sutch BT, Cai Q, Qin PZ, Haworth IS. Computation of nitroxide-nitroxide distances for spin-labeled DNA duplexes. Biopolymers 2007;87:40–50. [PubMed: 17538992]
40. Schiemann O, Weber A, Edwards TE, Prisner TF, Sigurdsson ST. Nanometer distance measurements on RNA using PELDOR. J Am Chem Soc 2003;125:3334–3335.
41. Edwards TE, Okonogi TM, Sigurdsson ST. Investigation of RNA-protein and RNA-metal ion interactions by electron paramagnetic resonance spectroscopy: The HIV TAR-Tat motif. Chem Biol 2002;9:699–706. [PubMed: 12079781]
42. Edwards TE, Sigurdsson ST. Electron paramagnetic resonance dynamic signatures of TAR RNA-small molecule complexes provide insight into RNA structure and recognition. Biochemistry 2002;41:14843–14847. [PubMed: 12475232]
43. Edwards TE, Sigurdsson ST. EPR spectroscopic analysis of TAR RNA-metal ion interactions. Biochem Biophys Res Commun 2003;303:721–725. [PubMed: 12659878]
44. Kim NK, Murali A, DeRose VJ. Separate metal requirements for loop interactions and catalysis in the extended hammerhead ribozyme. J Am Chem Soc 2005;127:14134–14135. [PubMed: 16218578]
45. Edwards TE, Sigurdsson ST. EPR spectroscopic analysis of U7 hammerhead ribozyme dynamics during metal ion induced folding. Biochemistry 2005;44:12870–12878. [PubMed: 16171402]
46. Ramos A, Varani G. A new method to detect long-range protein-RNA contacts: NMR detection of electron-proton relaxation induced by nitroxide spin-labeled RNA. J Am Chem Soc 1998;120:10992–10993.
47. Ramos A, Bayer P, Varani G. Determination of the structure of the RNA complex of a double-stranded RNA-binding domain from *Drosophila* Staufen protein. Biopolymers 1999;52:181–196. [PubMed: 11295750]
48. Ramos A, Grünert S, Adams J, Micklem DR, Proctor MR, Freund S, Bycroft M, St Johnston D, Varani G. RNA recognition by a Staufen double-stranded RNA-binding domain. EMBO J 2000;19:997–1009. [PubMed: 10698941]
49. Varani L, Gunderson SI, Mattaj IW, Kay LE, Neuhaus D, Varani G. The NMR structure of the 38 kDa U1A protein–PIE RNA complex reveals the basis of cooperativity in regulation of polyadenylation by human U1A protein. Nat Struct Biol 2000;7:329–335. [PubMed: 10742179]
50. Piton N, Schiemann O, Mu Y, Stock G, Prisner T, Engels JW. Synthesis of spin-labeled RNAs for long range distance measurements by peldor. Nucleosides Nucleotides Nucleic Acids 2005;24:771–775. [PubMed: 16248034]
51. Schiemann O, Piton N, Plackmeyer J, Bode BE, Prisner TF, Engels JW. Spin labeling of oligonucleotides with the nitroxide TPA and use of PELDOR, a pulse EPR method, to measure intramolecular distances. Nat Protoc 2007;2(4):904–923. [PubMed: 17446891]
52. Grant GPG, Qin PZ. A facile method for attaching nitroxide spin labels at the 5′-terminus of nucleic acids. Nucleic Acids Res 2007;35(10):e77. [PubMed: 17517787]
53. Macosko JC, Pio MS, Tinoco I Jr, Shin YK. A novel 5′ displacement spin-labeling technique for electron paramagnetic resonance spectroscopy of RNA. RNA 1999;5:1158–1166. [PubMed: 10496217]
54. Dugas H, Caron M. Specific spin-labeling of transfer ribonucleic acid molecules. Nucleic Acids Res 1976;3:19–34. [PubMed: 175353]
55. Toppin CR, Thomas IE, Bobst EV, Bobst AM. Synthesis of spin labelled deoxynucleotide analogues and their incorporation with terminal deoxynucleotidyl transferase into DNA. Int J Biol Macromol 1983;5:33–36.

56. Pauly GT, Thomas IE, Bobst AM. Base dynamics of nitroxide-labeled thymidine analogs incorporated into (dA-dT)n by DNA polymerase I from *E. coli*. Biochemistry 1987;26:7304–7310. [PubMed: 2827751]
57. Strobel OK, Keyes RS, Sinden RR, Bobst AM. Rigidity of a B–Z region incorporated into a plasmid as monitored by electron paramagnetic resonance. Arch Biochem Biophys 1995;324:357–366. [PubMed: 8554327]
58. Bobst AM, Pauly GT, Keyes RS, Bobst EV. Enzymatic sequence-specific spin labeling of a DNA fragment containing the recognition sequence of EcoRI endonuclease. FEBS Lett 1988;228:33–36. [PubMed: 2830135]
59. Xiao M, Martin I, Yablonovitch E, Jiang HW. Electrical detection of the spin resonance of a single electron in a silicon field-effect transistor. Nature 2004;430:435–439. [PubMed: 15269763]
60. Hustedt EJ, Beth AH. Nitroxide spin-spin interactions: Applications to protein structure and dynamics. Annu Rev Biophys Biomol Struct 1999;28:129–153. [PubMed: 10410798]
61. Hustedt, EJ.; Beth, AH. Structural information from CW-EPR spectra of dipolar coupled nitroxide spin labels. In: Berliner, LJ.; Eaton, GR.; Eaton, SS., editors. Biological Magnetic Resonance: Distance Measurements in Biological Systems by EPR. Kluwer Academic; New York: 2000. p. 155-184.
62. Hustedt EJ, Smirnov AI, Laub CF, Cobb CE, Beth AH. Molecular distances from dipolar coupled spin-labels: The global analysis of multifrequency continuous wave electron paramagnetic resonance data. Biophys J 1997;72:1861–1877. [PubMed: 9083690]
63. Mchaourab HS, Oh KJ, Fang CJ, Hubbell WL. Conformation of T4 lysozyme in solution. Hinge-bending motion and the substrate-induced conformational transition studied by site-directed spin labeling. Biochemistry 1997;36:307–316. [PubMed: 9003182]
64. Rabenstein MD, Shin YK. Determination of the distance between two spin labels attached to a macromolecule. Proc Natl Acad Sci 1995;92:8239–8243. [PubMed: 7667275]
65. Xiao, W.; Shin, YK. EPR spectroscopic ruler: The method and its applications. In: Berliner, LJ.; Eaton, GR.; Eaton, SS., editors. Biological Magnetic Resonance, Volume 19: Distance Measurements in Biological Systems by EPR. Kluwer Academic; New York: 2000. p. 249-276.
66. Altenbach C, Oh KJ, Trabanino RJ, Hideg K, Hubbell WL. Estimation of inter-residue distances in spin labeled proteins at physiological temperatures: Experimental strategies and practical limitations. Biochemistry 2001;40:15471–15482. [PubMed: 11747422]
67. Steinhoff HJ, Radzwill N, Thevis W, Lenz V, Brandenburg D, Antson A, Dodson G, Wollmer A. Determination of interspin distances between spin labels attached to insulin: Comparison of electron paramagnetic resonance data with the X-ray structure. Biophys J 1997;73:3287–3298. [PubMed: 9414239]
68. Schweiger, A.; Jeschke, G. Principles of Pulse Electron Paramagnetic Resonance. Oxford University Press; Oxford: 2001.
69. Borbat, PP.; Freed, JH. Double-quantum ESR and distance measurements. In: Berliner, LJ.; Eaton, GR.; Eaton, SS., editors. Biological Magnetic Resonance, Volume 19: Distance Measurements in Biological Systems by EPR. Kluwer Academic; New York: 2000. p. 383-459.
70. Milov AD, Salikohov KM, Shirov MD. Applications of ENDOR in electron-spin echo for paramagnetic center space distribution in solids. Fiz Tverd Tela 1981;23:975–982.
71. Kurshev VV, Raitsimring AM, Tsvetkov YD. Selection of dipolar interaction by the “2 + 1” pulse train ESE. J Magn Reson 1989;81(3):441–454.1969
72. Milov AD, Ponomarev AB, Tsvetkov YD. Electron-electron double resonance in electron spin echo: Model biradical systems and the sensitized photolysis of decalin. Chem Phys Lett 1984;110(1):67–72.
73. Larsen RG, Singel DJ. Double electron—electron resonance spin—echo modulation: Spectroscopic measurement of electron spin pair separations in orientationally disordered solids. J Chem Phys 1993;98(7):5134–5146.
74. Rakowsky MH, More KM, Kulikov AV, Eaton GR, Eaton SS. Time-domain electron paramagnetic resonance as a probe of electron-electron spin-spin interaction in spin-labeled low-spin iron porphyrins. J Am Chem Soc 1995;117(7):2049–2057.

75. Saxena S, Freed JH. Double quantum two-dimensional Fourier transform electron spin resonance: Distance measurements. Chem Phys Lett 1996;251(1–2):102–110.
76. Saxena S, Freed JH. Theory of double quantum two-dimensional electron spin resonance with application to distance measurements. J Chem Phys 1997;107:1317–1340.
77. Martin RE, Pannier M, Diederich F, Gramlich V, Hubrich M, Spiess HW. Determination of end-to-rnd distances in a series of TEMPO diradicals of up to 2.8 nm length with a new four-pulse double electron electron resonance experiment. Angew Chem Int Ed 1998;37(20):2834–2837.
78. Borbat PP, Freed JH. Multiple-quantum ESR and distance measurements. Chem Phys Lett 1999;313:145–154.
79. Pannier M, Veit S, Godt A, Jeschke G, Spiess HW. Dead-time free measurement of dipole-dipole interactions between electron spins. J Magn Res 2000;142:331–340.
80. Schiemann O, Prisner TF. Long-range distance determinations in biomacromolecules by EPR spectroscopy. Q Rev Biophys 2007;40:1–53. [PubMed: 17565764]
81. Borbat PP, Davis JH, Butcher SE, Freed JH. Measurement of large distances in biomolecules using double-quantum filtered refocused electron spin-echoes. J Am Chem Soc 2004;126:7746–7747. [PubMed: 15212500]
82. Grant GPG, Popova A, Qin PZ. Diastereomer characterizations of nitroxide-labeled nucleic acids. Biochem Biophys Res Commun 2008;371:451–455. [PubMed: 18442474]
83. Ward R, Keeble DJ, El-Mkami H, Norman DG. Distance determination in heterogeneous DNA model systems by pulsed EPR. Chem Bio Chem 2007;8:1957–1964.
84. Jeschke, G.; Pannier, M.; Spiess, HW. Double electron-electron resonance: Methodical advances and application to disordered systems. In: Berliner, LJ.; Eaton, GR.; Eaton, SS., editors. Biological Magnetic Resonance, Volume 19: Distance Measurements in Biological Systems by EPR. Kluwer Academic; New York: 2000. p. 493-512.
85. Jeschke G, Panek G, Godt A, Bender A, Paulsen H. Data analysis procedures for pulse ELDOR measurements of broad distance distributions. Appl Magn Reson 2004;26:223–244.
86. Bowman MK, Maryasov AG, Kim N, DeRose VJ. Visulation of distance distribution from pulsed double electron-electron resonance data. Appl Magn Reson 2004;26:23–39.
87. Sale K, Song L, Liu YS, Perozo E, Fajer P. Explicit treatment of spin labels in modeling of distance constraints from dipolar EPR and DEER. J Am Chem Soc 2005;127:9334–9335. [PubMed: 15984837]
88. Darian E, Gannett PM. Application of molecular dynamics simulations to spin-labeled oligonucleotides. J Biomol Struct Dyn 2005;22:579–593. [PubMed: 15702930]
89. Griffith, HO.; Jost, PC. Lipid spin labels in biological membranes. In: Berliner, LJ., editor. Spin Labeling Theory and Application. Academic Press; New York: 1976. p. 453-423.
90. Mchaourab HS, Lietzow MA, Hideg K, Hubbell WL. Motion of spin-labeled side chains in T4 lysozyme. Correlation with protein structure and dynamics. Biochemistry 1996;35:7692–7704. [PubMed: 8672470]
91. Hubbell WL, Mchaourab HS, Altenbach C, Lietzow MA. Watching proteins move using site-directed spin labeling. Structure 1996;4:779–783. [PubMed: 8805569]
92. Robinson BH, Slusky LJ, Auteri FP. Direct simulation of continuous wave electron paramagnetic resonance spectra from Brownian dynamics trajectories. J Chem Phys 1992;96:2609–2616.
93. Steinhoff HJ, Hubbell WL. Calculation of electron paramagnetic resonance spectra from Brownian dynamics trajectories: Application to nitroxide side chains in proteins. Biophys J 1996;71:2201–2212. [PubMed: 8889196]
94. Budil DE, Sale KL, Khairy KA, Fajer PG. Calculating slow-motional electron paramagnetic resonance spectra from molecular dynamics using a diffusion operator approach. J Phys Chem A 2006;110:3703–3713. [PubMed: 16526654]
95. Fajer MI, Li H, Yang W, Fajer PG. Mapping electron paramagnetic resonance spin label conformations by the simulated scaling method. J Am Chem Soc 2007;129:13840–13846. [PubMed: 17948993]
96. Moro G, Freed JH. Efficient computation of magnetic resonance spectra and related correlation functions from stochastic Liouville equations. J Phys Chem 1980;84:2837–2840.

97. Hustedt EJ, Spaltenstein A, Kirchner JJ, Hopkins PB, Robinson BH. Motions of short DNA duplexes: An analysis of DNA dynamics using an EPR-active probe. Biochemistry 1993;32:1774–1787. [PubMed: 8382521]

98. Schneider, DJ.; Freed, JH. Calculating slow motional magnetic resonance spectra: A user's guide. In: Berliner, LJ., editor. Spin Labeling: Theory and Applications. Plenum Press; New York: 1989. p. 1-76.

99. Budil DE, Lee S, Saxena S, Freed JH. Nonlinear-least-squares analysis of slow-motion EPR spectra in one and two dimensions using a modified Levenberg-Marquardt algorithm. J Mag Res Series A 1996;120:155–189.

100. Liang Z, Freed JH. An assessment of the applicability of multifrequency ESR to study the complex dynamics of biomolecules. J Phys Chem B 1999;103:6384–6396.

101. Liang Z, Freed JH, Keyes RS, Bobst AM. An electron spin resonance study of DNA dynamics using the slowly relaxing local structure model. J Phys Chem 2000;104:5372–5381.

102. Qin PZ, Jennifer I, Oki A. A model system for investigating lineshape/structure correlations in RNA site-directed spin labeling. Biochem Biophys Res Commun 2006;343:117–124. [PubMed: 16530169]

103. Columbus L, Kalai T, Jeko J, Hideg K, Hubbell WL. Molecular motion of spin-labeled side chains in α-helices: Analysis by variation of side chain structure. Biochemistry 2001;40:3828–3846. [PubMed: 11300763]

104. Okonogi TM, Reese AW, Alley SC, Hopkins PB, Robinson BH. Flexibility of duplex DNA on the submicrosecond timescale. Biophys J 1999;77:3256–3276. [PubMed: 10585948]

105. Okonogi TM, Alley SC, Reese AW, Hopkins PB, Robinson BH. Sequence-dependent dynamics of duplex DNA: The applicability of a dinucleotide model. Biophys J 2002;83:3446–3459. [PubMed: 12496111]

106. Okonogi TM, Alley SC, Reese AW, Hopkins PB, Robinson BH. Sequence-dependent dynamics in duplex DNA. Biophys J 2000;78:2560–2571. [PubMed: 10777752]

107. Cantor, CR.; Schimmel, PR. Biophysical Chemistry. W.H. Freeman; San Francisco: 1980. p. 460-564.

108. Hester JD, Bobst EV, Kryak DD, Bobst AM. Identification of a single genome by electron paramagnetic resonance (EPR) with nitroxide-labeled oligonucleotide probes. Free Radic Res 2002;36:491–498. [PubMed: 12150537]

109. Keyes RS, Bobst EV, Cao YY, Bobst AM. Overall and internal dynamics of DNA as monitored by five-atom-tethered spin labels. Biophys J 1997;72:282–290. [PubMed: 8994613]

110. Okonogi TM, Alley SC, Harwood EA, Hopkins PB, Robinson BH. Phosphate backbone neutralization increases duplex DNA flexibility: A model for protein binding. Proc Natl Acad Sci 2002;99:4156–4160. [PubMed: 11929991]

111. Spaltenstein A, Robinson BH, Hopkins PB. Sequence- and structure-dependent DNA base dynamics: Synthesis, structure, and dynamics of site and sequence specifically spin-labeled DNA. Biochemistry 1989;28:9484–9495. [PubMed: 2558721]

112. Allain FHT, Varani G. Structure of the P1 helix from group I self-splicing introns. J Mol Biol 1995;250:333–353. [PubMed: 7608979]

113. Akke M, Fiala R, Jiang F, Patel D, Palmer AG. Base dynamics in a UUCG tetraloop RNA hairpin characterized by 15N spin relaxation: Correlations with structure and stability. RNA 1997;3:702–709. [PubMed: 9214654]

114. Qin PZ, Feigon J, Hubbell WL. Site-directed spin labeling studies reveal solution conformational changes in a GAAA tetraloop receptor upon Mg^{2+}-dependent docking of a GAAA tetraloop. J Mol Biol 2005;351:1–8. [PubMed: 15993422]

115. Cate JH, Gooding AR, Podell E, Zhou K, Golden BL, Kundrot CE, Cech TR, Doudna JA. Crystal structure of a group I ribozyme domain: Principles of RNA packing. Science 1996;273(5282):1678–1685. [PubMed: 8781224]

116. Frankel AD, Young JAT. HIV-1: Fifteen proteins and an RNA. Annu Rev Biochem 1998;67:1–25. [PubMed: 9759480]

117. Edwards TE, Robinson BH, Sigurdsson ST. Identification of amino acids that promote specific and rigid TAR RNA-Tat protein complex formation. Chem Biol 2005;12:329–337. [PubMed: 15797217]

118. Blount KF, Uhlenbeck OC. The structure-function dilemma of the hammerhead ribozyme. Annu Rev Biophys Biomol Struct 2005;34:415–440. [PubMed: 15869397]

119. Shin YK, Hubbell WL. Determination of electrostatic potentials at biological interfaces using electron-electron double resonance. Biophys J 1992;61:1443–1453. [PubMed: 1319760]

120. Nielsen RD, Canaan S, Gladden JA, Gelb MH, Mailer C, Robinson BH. Comparing continuous wave progressive saturation EPR and time domain saturation recovery EPR over the entire motional range of nitroxide spin labels. J Mag Res 2004;16:129–163.

121. Smirnova TI, Chadwick TG, Voinov MA, Poluektov O, van Tol J, Ozarowski A, Schaaf G, Ryan MM, Bankaitis VA. Local polarity and hydrogen bonding inside the Sec14p phospholipid-binding cavity: High-field multi-frequency electron paramagnetic resonance studies. Biophys J 2007;92:3686–3695. [PubMed: 17325006]

122. Clore GM, Tang C, Iwahara J. Elucidating transient macromolecular interactions using paramagnetic relaxation enhancement. Curr Opin Struct Biol 2007;17:603–616. [PubMed: 17913493]

123. Leulliot N, Quevillon-Cheruel S, Graille M, van Tilbeurgh H, Leeper TC, Godin KS, Edwards TE, Sigurdsson ST, Rozenkrants N, Nagel RJ, Ares M Jr, Varani G. A new alpha-helical extension promotes RNA binding by the dsRBD of Rnt1p RNAse III. EMBO J 2004;23:2468–2477. [PubMed: 15192703]

124. DeRose VJ. Metal ion binding to catalytic RNA molecules. Curr Opin Struct Biol 2003;13:317–324. [PubMed: 12831882]

125. Hoogstraten CG, Grant CV, Horton TE, DeRose VJ, Britt RD. Structural analysis of metal ion ligation to nucleotides and nucleic acids using pulsed EPR spectroscopy. J Am Chem Soc 2002;124:834–842. [PubMed: 11817959]

126. Horton TE, Clardy DR, DeRose VJ. Electron paramagnetic resonance spectroscopic measurement of Mn^{2+} binding affinities to the hammerhead ribozyme and correlation with cleavage activity. Biochemistry 1998;37:18094–18101. [PubMed: 9922178]

127. Morrissey SR, Horton TE, Grant CV, Hoogstraten CG, Britt RD, DeRose VJ. Mn^{2+}-nitrogen interactions in RNA probed by electron spin-echo envelope modulation spectroscopy: Application to the hammerhead ribozyme. J Am Chem Soc 1999;121:9215–9218.

128. Morrissey SR, Horton TE, DeRose VJ. Mn^{2+} sites in the hammerhead ribozyme investigated by EPR and continuous-wave Q-band ENDOR spectroscopies. J Am Chem Soc 2000;122:3473–3481.

129. Schiemann O, Fritscher J, Kisseleva N, Sigurdsson ST, Prisner TF. Structural investigation of a high-affinity MnII binding site in the hammerhead ribozyme by EPR spectroscopy and DFT calculations. Effects of neomycin B on metal-ion binding. Chembiochem 2003;4:1057–1065. [PubMed: 14523924]

130. Kisseleva N, Khvorova A, Westhof E, Schiemann O. Binding of manganese(II) to a tertiary stabilized hammerhead ribozyme as studied by electron paramagnetic resonance spectroscopy. RNA 2005;11:1–6. [PubMed: 15611296]

131. Vogt M, Lahiri S, Hoogstraten CG, Britt RD, DeRose VJ. Coordination environment of a site-bound metal ion in the hammerhead ribozyme determined by 15N and 2H ESEEM spectroscopy. J Am Chem Soc 2006;128:16764–16770. [PubMed: 17177426]

132. Schiemann O, Carmieli R, Goldfarb D. W-band 31P-ENDOR on the high-affinity Mn^{2+} binding site in the minimal and tertiary stabilized hammerhead ribozymes. Appl Magn Reson 2007;31:543–552.

133. Butcher SE, Dieckmann T, Feigon J. Solution structure of a GAAA tetraloop receptor RNA. EMBO J 1997;16:7490–7499. [PubMed: 9405377]

134. LaConte LEW, Voelz V, Nelson W, Enz M, Thomas DD. Molecular dynamics simulation of site-directed spin labeling: Experimental validation in muscle fibers. Biophys J 2002;83:1854–1866. [PubMed: 12324407]

135. Stoica I. Using Molecular dynamics to simulate electronic spin resonance spectra of T4 lysozyme. J Phys Chem B 2004;108:1771–1782.

136. Beier C, Steinhoff HJ. A structure-based simulation approach for electron paramagnetic resonance spectra using molecular and stochastic dynamics simulations. Biophys J 2006;91:2647–2664. [PubMed: 16844740]

137. DeSensi SC, Rangel DP, Beth AH, Lybrand TP, Hustedt EJ. Simulation of nitroxide electron paramagnetic resonance spectra from Brownian trajectories and molecular dynamics simulations. Biophys J 2008;94:3798–3809. [PubMed: 18234808]

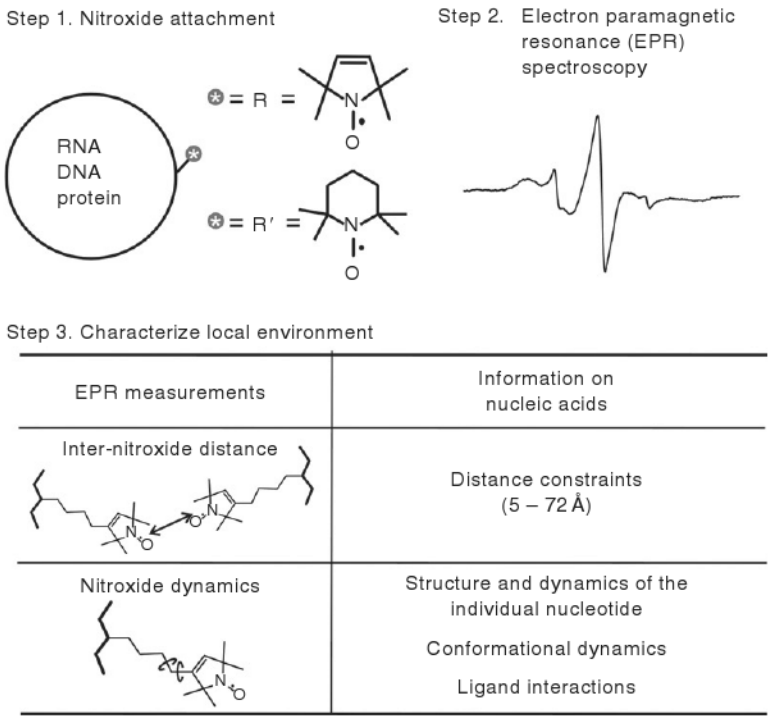

Fig. 1.

The general strategy of site-directed spin labeling (SDSL). The first step in SDSL is to covalently attach nitroxides (yellow star)to specific sites of a macromolecule. The chemical structures of the two most commonly used nitroxides (*R* and *R′*) are shown. In step 2, EPR spectroscopy is used to monitor the behavior of the nitroxide. In step 3,the nitroxide behavior is used to obtain information on the local environment of the labeling site(s). The table shows the two types of EPR measurements that serve as the primary source of information in nucleic acid SDSL studies.

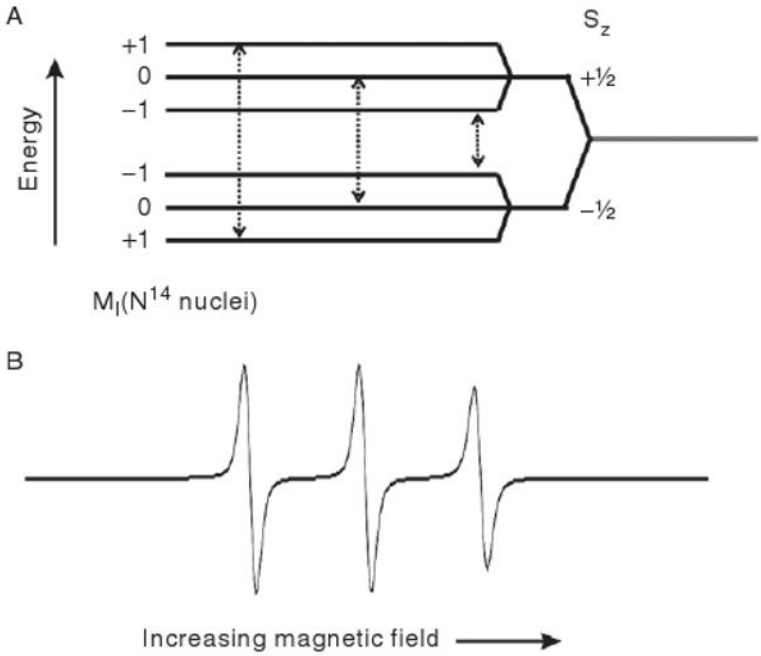

Fig. 2.

Electron spin energy level diagram and the continuous-wave EPR spectrum. (A) A schematic of the energy levels of an electron spin. In the absence of an applied magnetic field, the energy levels corresponding to the two electron spin states ($S_z = \pm 1/2$) are degenerate (purple line). In the presence of an applied magnetic field, the electron energy levels separate according to the spin quantum number S_z (the Zeeman effect) and the nuclear spin quantum number M_I (the hyperfine interaction). (B) A representative EPR spectrum. The spectrum is obtained by varying the applied magnetic field strength at a fixed microwave frequency, and is shown as the first derivative of the absorption spectrum. The three peaks correspond to the three transitions indicated by the dotted arrows in the energy diagram shown in (A).

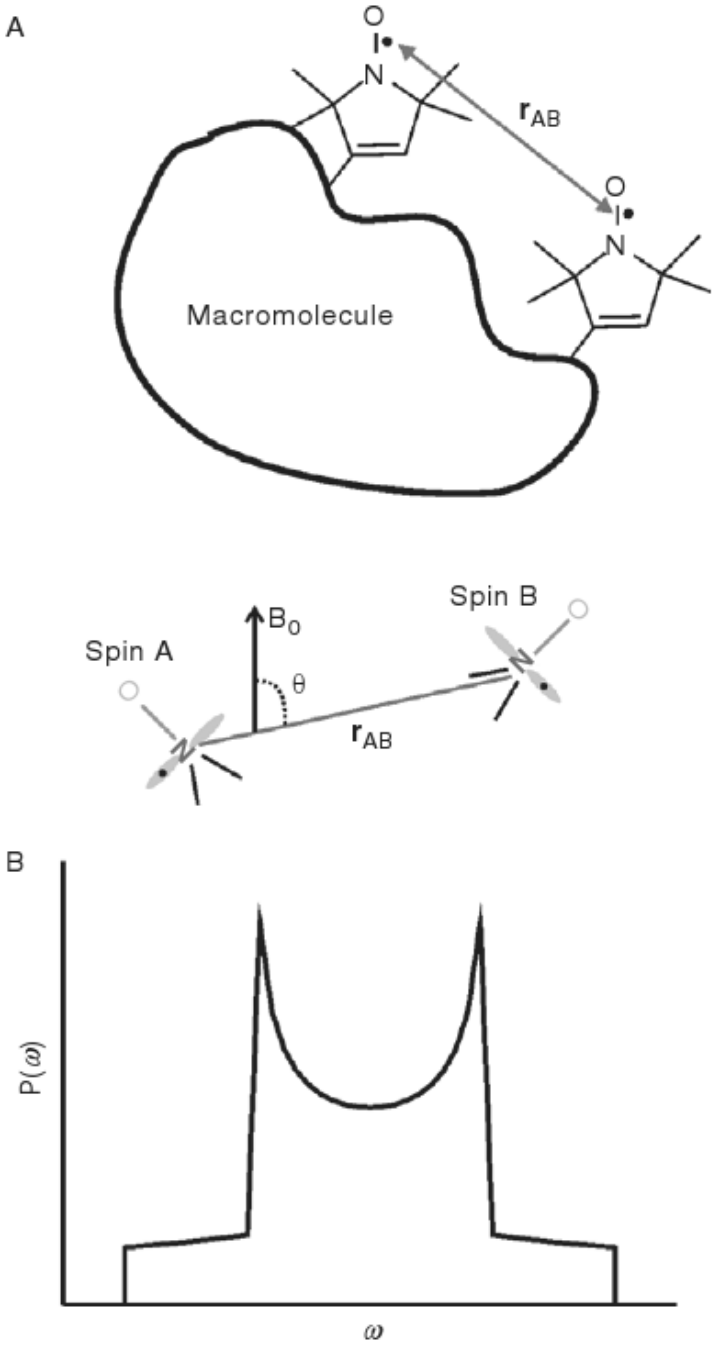

Fig. 3.

Dipolar coupling between a pair of electron spins. (A) Schematic diagrams illustrating the attachment of two nitroxides to a macromolecule and the relationship between the distance vector ($\mathbf{r_{AB}}$) and the magnetic field vector ($\mathbf{B_0}$). (B) A Pake pattern illustrating the probability distribution of the dipolar interaction energy expressed in terms of the angular frequency ω. This Pake pattern represents the case where the distance vector adopts a static and isotropic distribution with respect to the magnetic field vector.

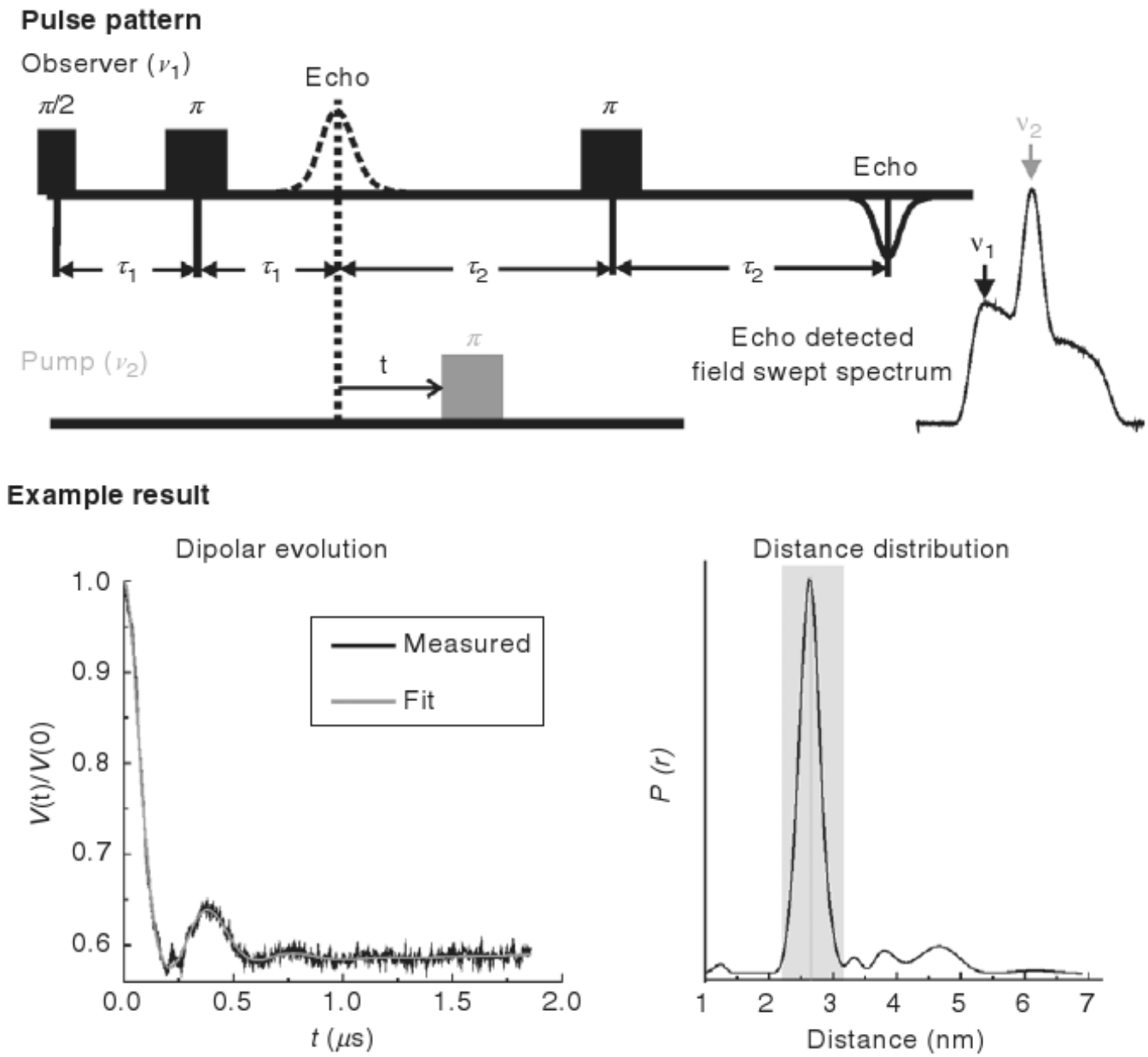

Fig. 4.

Double electron-electron resonance (DEER) spectroscopy. Shown on top is the pulse sequence for the four-pulse DEER. Shown at the bottom is a set of DEER data measured in a dodecameric DNA duplex (35). The DEER measurement gives an average distance $\langle r_{DEER} \rangle$ = 26.4 Å. The standard deviation (σ_{DEER}), which characterizes the width of the distance distribution, is 1.7 Å. The predicted distance, computed using the NASNOX, is $\langle r_{NASNOX} \rangle$ = 26.8 Å and $\langle \sigma_{NASNOX} \rangle$ = 2.8 Å (35). Reproduced from references (35,37) with permission.

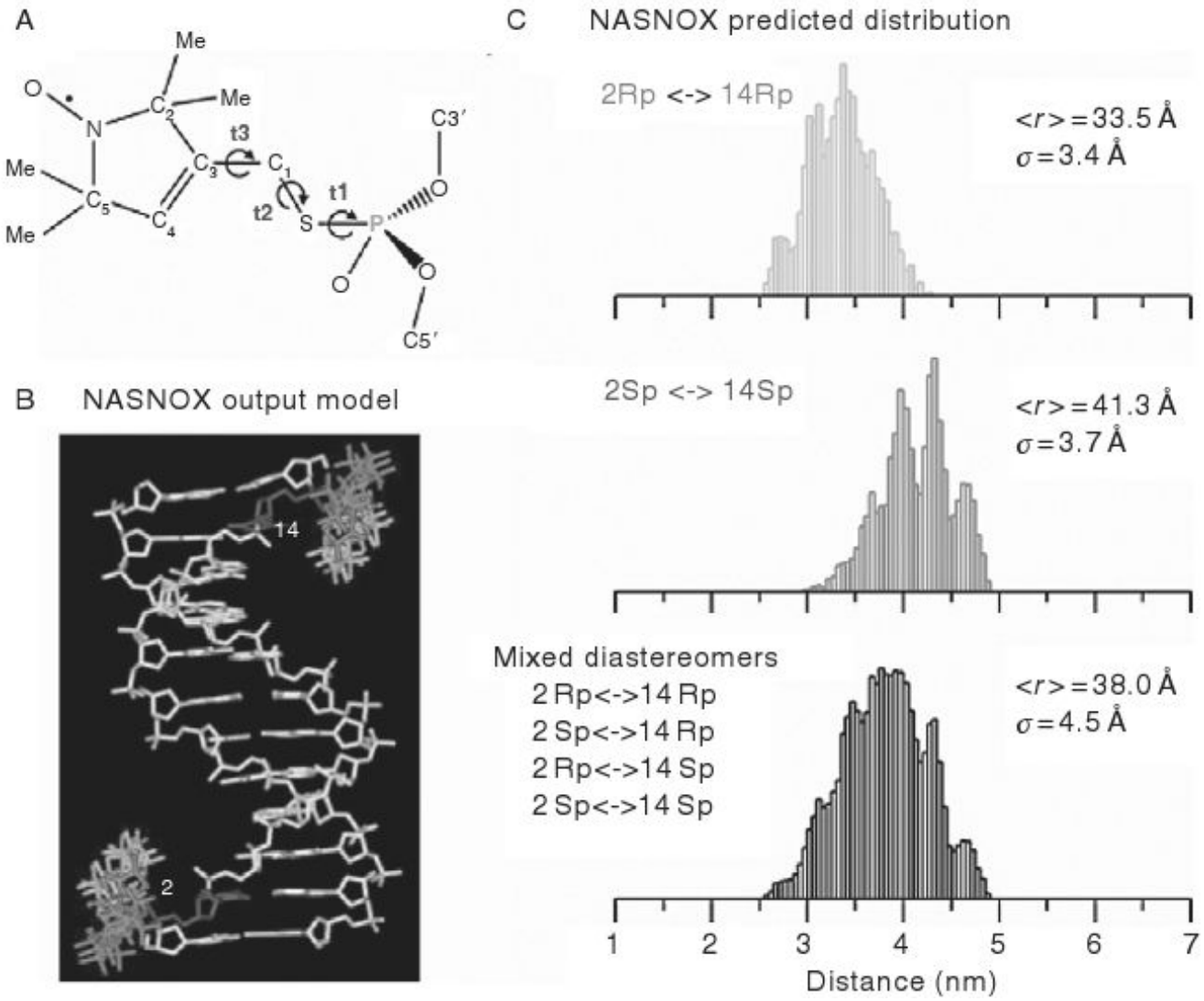

Fig. 5.

The NASNOX program for predicting inter-R5 distances. (A) A schematic of the R5 nitroxide probe. The configuration shown is the R_p diastereomer. The three torsion angles (t1, t2, and t3) that are varied in the conformer search are marked. (B) An example of structural output from NASNOX. Shown as colored sticks are the predicted allowable R5 conformers at two sites near the termini of a dodecameric DNA duplex. At each site, nitroxides attached to the R_p diastereomer are shown in green, and nitroxides attached to the S_p diastereomer are shown in red. (C) The predicted internitroxide distance distribution obtained from the output structure shown in (B). The DEER measurement using mixed diastereomers gave a $\langle r_{DEER} \rangle$ of 38.8 Å (35), which is consistent with the NASNOX prediction of $\langle r \rangle$ = 38.0 Å. Data reproduced from (35) with permission.

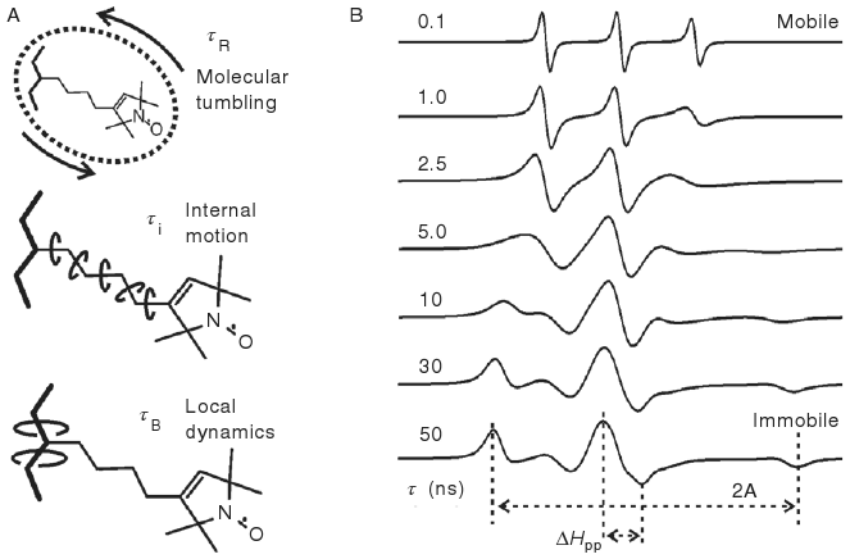

Fig. 6.

The relationship between nitroxide dynamics and cw-EPR spectral lineshapes. (A) The three modes of motion that contribute to nitroxide dynamics. (B) Simulated X-band EPR spectra of nitroxides undergoing isotropic rotation at different rotational correlation time τ.

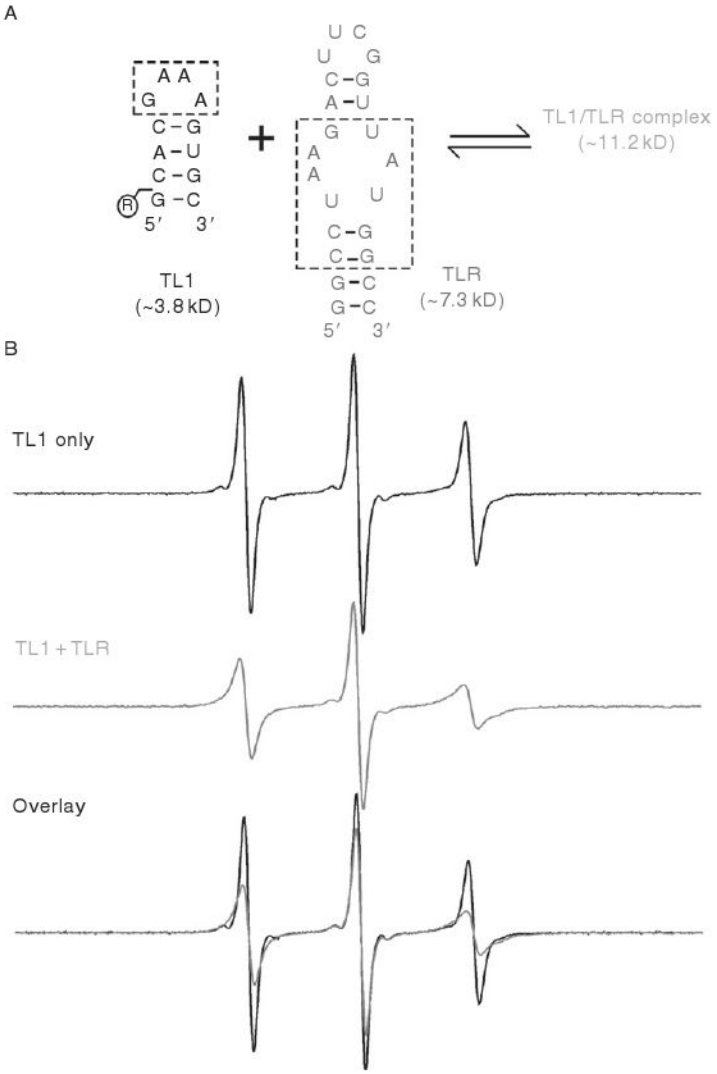

Fig. 7.

SDSL studies of GAAA tetraloop binding to its RNA receptor. (A) A schematic diagram illustrating the experimental design. Shown in black is a 12-nt RNA hairpin (TL1) containing the GAAA tetraloop (boxed). The TL1 RNA was labeled with the phosphorothioate scheme (Table I, entry 1), with the labeling site represented by R. Shown in purple is a 23-nt RNA (TLR), which contains the 11-nt RNA receptor (boxed) for the GAAA tetraloop. (B) EPR spectra of the free and bound TL1. The spectra shown were normalized to the same number of spins. For TL1 by itself, the spectrum in aqueous solution (black) shows three sharp lines, consistent with that of a molecule undergoing fast tumbling. On formation of the TL1/TLR complex, the spectrum (red) shows a clear reduction in magnitude of the high-field line as well as broadening of all three lines, indicating a reduction in nitroxide dynamics. The change in nitroxide dynamics reflects a reduction in the overall tumbling rate due to the formation of the TL1/TLR complex with a higher molecular weight. Data reproduced from reference (22) with permission.

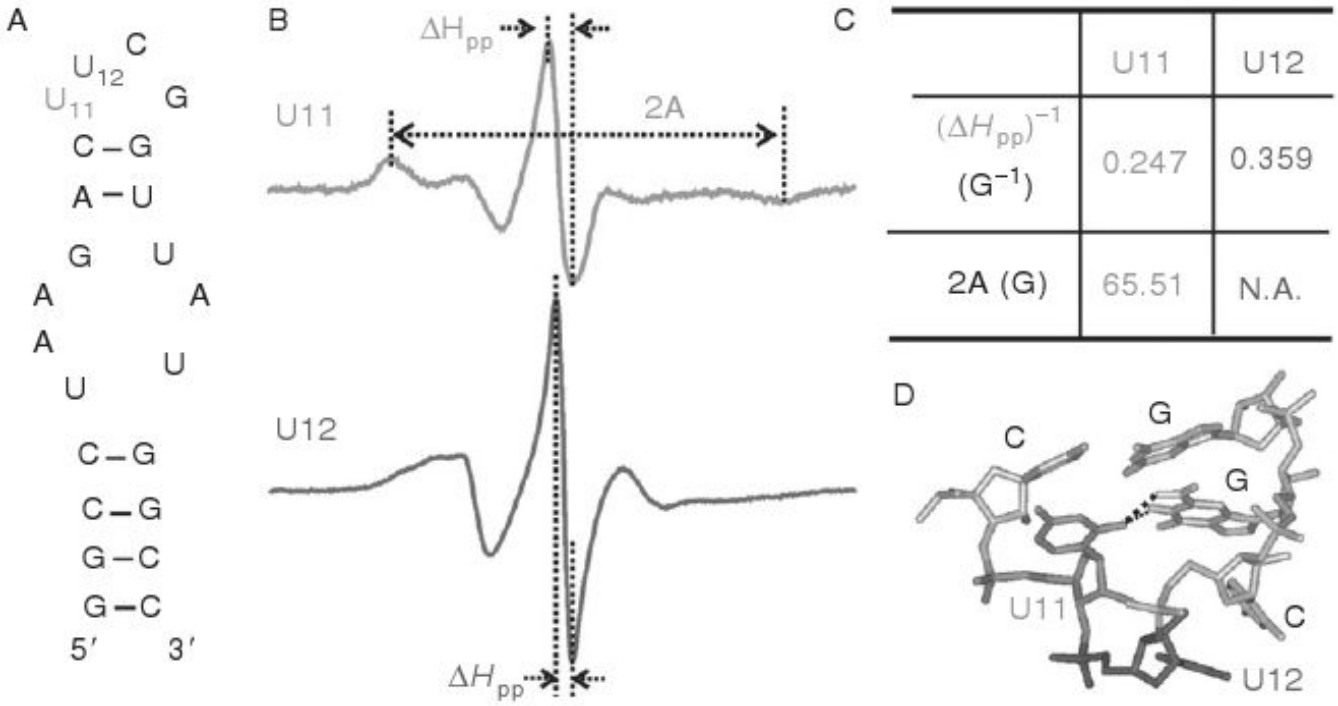

	U11	U12
$(\Delta H_{pp})^{-1}$ (G^{-1})	0.247	0.359
2A (G)	65.51	N.A.

Fig. 8.

SDSL studies of a UUCG loop. (A) The sequence and secondary structure of the TLR RNA. The two uridines within the UUCG loop are colored blue and red, respectively. (B) EPR spectra of nitroxides attached to U11 (red) and U12 (blue). The nitroxides were attached to the respective uridine base using the 4-thioU scheme (Table I, entry 3a). (C) Semiquantitative analysis of the spectra shown in (B). The EPR spectrum of U11 (red) shows broad centerline [large ΔH_{pp} and small $(\Delta H_{pp})^{-1}$] and large hyperfine splitting (2A), indicating a nitroxide with limited mobility. The spectrum for U12 shows narrow centerline [small ΔH_{pp} and large $(\Delta H_{pp})^{-1}$] and no clear hyperfine splitting, indicating a mobile nitroxide. (D) The NMR structure of the UUCG loop (112). The structure shows that U11 is hydrogen-bonded (dotted lines) and stacked, while U12 is structurally unrestrained. Data reproduced with permission from (31).

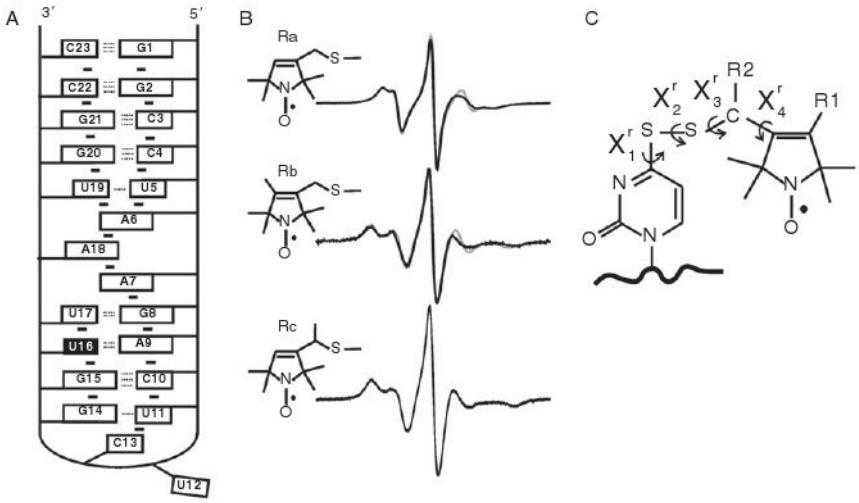

Fig. 9.

Nitroxide motion at U16 of the TLR RNA. (A) A schematic of the sequence and secondary structure of the TLR RNA. The U16 base is shown in black. (B) EPR spectra of three variants of nitroxide (Ra, Rb, Rc) attached to the U16 base using the 4-thioU scheme. The experimental spectra are shown in black, and spectra simulated using MOMD are shown in red. (C) The chemical structure of the Rx series of spin labels. The designations of various atoms and dihedral angles are shown. Data reproduced with permission from (31).

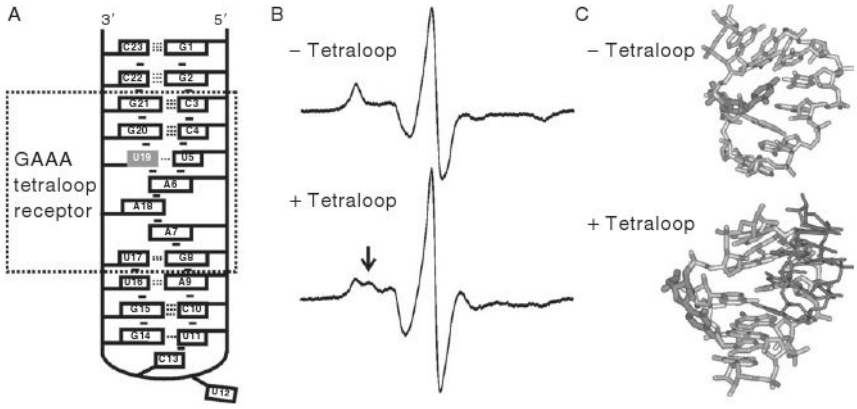

Fig. 10.

Conformational changes in the GAAA tetraloop receptor upon tetraloop docking. (A) A schematic diagram showing the secondary structure of the TLR RNA. The GAAA tetraloop receptor is indicated by the box. The U19 base is shown in red. (B) EPR spectra at the U19 site. The nitroxide is attached to the U19 base using the 4-thioU scheme. The arrow indicates a mobile component that appears upon tetraloop-receptor interaction. Due to the weak affinity between the isolated tetraloop and receptor in solution, the "+ Tetraloop" spectrum is a composite of the bound and unbound receptors. (C) Structures of the unbound and bound receptor. Shown on top is the NMR structure of the unbound receptor (133), and shown at the bottom is the crystal structure of the tetraloop/receptor complex as observed in the P456 domain of group I intron *Tetrahynema* (115). In the unbound receptor (top), the U19 base (thick red line) is hydrogen-bonded and stacked within the helix. In the bound receptor (bottom), the U19 base (thick red line) is flipped out of the helix. Data reproduced from (114) with permission.

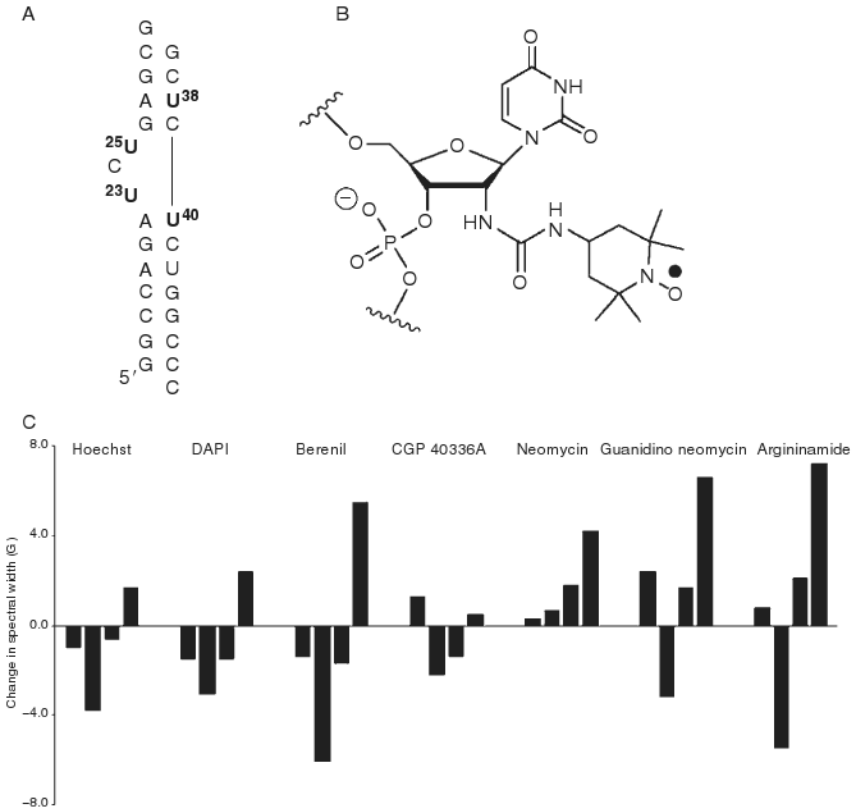

Fig. 11.

EPR dynamic signatures in the TAR RNA. (A) The TAR RNA construct used in SDSL studies. The nitroxide-labeled uridine nucleotides are shown in bold. (B) A schematic of a nitroxide covalently linked to the 2′-position of a uridine nucleotide in RNA (23). (C) The dynamic signatures of TAR RNA complexed with small molecule inhibitors (42). Changes in spectral width (2A) are plotted as a function of nucleotide position (U23, U25, U38, and U40) for each compound. An increase in spectral width corresponds to a decrease in nitroxide mobility and a decrease in spectral width corresponds to an increase in nitroxide mobility. Molecules that bind in a similar fashion, such as Hoechst, DAPI, and berenil, show similar dynamic signatures, whereas different patterns of the dynamic signature are observed for molecules that bind differently. Reproduced from (9) with permission.

Table I

Summary of Nitroxide Labeling Schemes that Use Solid-Phase Chemical Synthesis

Nitroxide attachment site	Examples of chemical structure	References
1 Phosphate	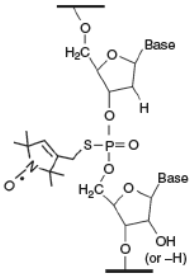	[22]
2 Sugar: 2′-position	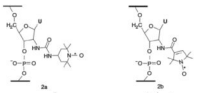	[23,24]
3 Base: 4-position of uridine	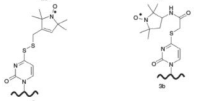	[31,46]
4 Base: acetylene linkage	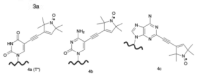	[27,30,32, 34]
5 Base: 5-position of pyrimidines with variable tethers (2-11 atom)	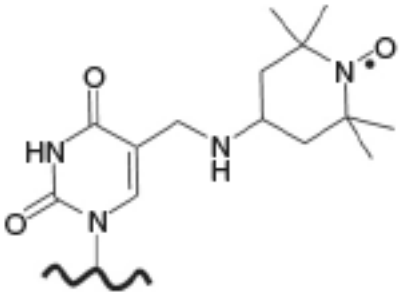 5a 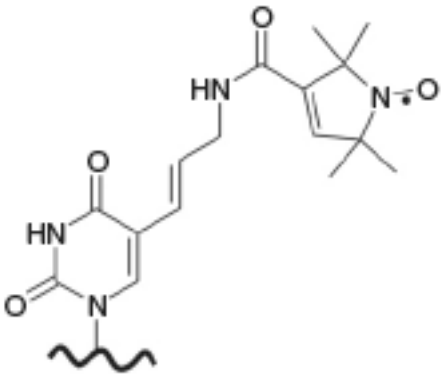 5b	[11]
6 Fused base		[28,33]